



<b>Document Type</b>		<b>Identification No.</b>	
Final Report		GTL-52-1-TR.2	
<b>No. of Pages</b>	48	<b>Revision</b>	0
<b>No. of Figures</b>	21	<b>Date of Issue</b>	Jun 87

An Engineering Study to Define  
Equipment for Full Scale Testing  
of Wind Resistance of  
Roofing Systems

Prepared for:  
Single Ply Roofing Institute

Prepared by:

  
R.J. Kind, P. Eng., M.D. Imray, D. Peloso

1011 Polytek Street, Gloucester, Ontario, K1J 8Z1  
744-3530

Table of Contents

## Table of Contents

	<u>page</u>
Abstract	
List of Symbols	
1. Introduction	1
2. Background Discussion	2
3. Apparatus and Test Procedures	5
4. Results	8
4.1 Open Jet Configurations	8
4.2 Enclosed Jet Configurations	10
4.3 Configurations With A Divider Plate	11
5. Recommendations and Cost Estimates	14
5.1 Recommended Open Jet Configuration	14
5.2 Recommended Enclosed Jet Configuration	15
5.3 Cost Estimates for Recommended Open Jet Configuration	17
6. Discussion	21
7. Conclusions	23
References	24
Tables	25
Figures	27
Appendix	48

## Abstract

This report is concerned with a study to find the optimum configuration for a full-scale test-rig to test the capability of roofing systems to withstand damage by high winds. The requirements that such a rig should satisfy are discussed.

A variety of configurations were tested at reduced scale, using a specially designed apparatus. Both open jet and enclosed jet configurations were examined. An open jet configuration is identified as the optimum. A rig that would satisfy the ideal requirements would be very large, would require a great deal of power (about 65,000 horsepower) and would be very costly. Some compromise on pressure-pattern size and maximum attainable wind speed will most probably be necessary.

List of Symbols

### List of Symbols

- A pressure pattern size parameter; see Chapter 2
- Cp non-dimensional pressure coefficient;  
 $C_p = (p - p_{atm}) / 0.5\rho V^2$ ;  
V =  $V_1$  for open jet configurations;  
V =  $V_2$  for closed jet configurations
- h jet height
- H height of test platform
- p actual static pressure at any point on test platform
- $p_{atm}$  atmospheric pressure
- P power
- V wind speed produced by test rig; subscripts 1 and 2 denote upstream and above test platform respectively - see Figure 19 for open jet and Figure 16 for enclosed jets.
- w jet width
- $\beta$  vortex generator angle; see Figure 2
- $\eta$  propeller efficiency
- $\rho$  density of sea-level atmospheric air

CHAPTER 1  
Introduction

1. Introduction

GasTOPS Ltd. has been contracted by the Single Ply Roofing Institute (SPRI) to carry out an engineering study to analyze what methods and type of equipment would be required to test the abilities of a wide range of roofing systems to withstand high winds.

This document constitutes the final report on that study. The approach used in the study was to test a large variety of possible test-rig configurations at small scale, using an apparatus specially designed for that purpose. Promising configurations were singled out for detailed investigation until the most cost-effective configurations that would give satisfactory results were found. Two configurations, one open and the other with an enclosure around the jet of wind are considered in detail. The open jet configuration appears most attractive and is recommended. Rough cost estimates are provided.



CHAPTER 2  
Background Discussion

2. Background Discussion

As explained in the literature [1, 2], and in the proposal [3], failure of inverted roofing systems involves dynamic flow processes. Traditional test methods, which involve application of a static pressure difference across the system, do not adequately simulate these processes and therefore cannot be expected to give valid results for all types of systems. It is considered essential that the test rig produce a high-speed flow of wind over the test platform and that the flow pattern be basically the same as that which prevails on actual rooftops when the wind is blowing. Wind tunnel tests have established that the critical case is when the wind direction is about 45° to the building walls, and that failure is most likely to occur near the upwind corner of the rooftop. The test rig must therefore simulate this situation, which is sketched in Figure 1. The general appearance of the test rig is expected to be as sketched in Figure 2.

The most costly components of the test rig would be the aircraft engines and propellers because high-power engines will be necessary. For example, about 10000 Horsepower would be required to produce a 10 ft x 13.5 ft jet of wind moving at 150 mph.

Therefore, it is essential to minimize the cross-section area of the required jet of wind. More precisely, the ratio

$$R_1 = \frac{\text{cross section area of jet of wind}}{\text{size of roofing system sample}} \quad (1.1)$$

must be as small as possible.

As already mentioned, the upwind-corner region of a rooftop is most sensitive to wind damage. The size of the critical region depends on the size and shape of the building and on parapet height. Various loose-laid roofing systems have been tested for Dow Chemical Inc. in wind tunnels at the National Research Council of Canada [3, 4]. These systems were installed on low-rise, intermediate-rise and high-rise building shapes. The height, width and length dimensions (in feet) of these buildings were as follows: 15 x 53 x 77; 45 x 45 x 45; 45 x 45 x 90; 75 x 30 x 60. These building dimensions can be considered reasonably representative for present purposes, and, as it happens, all of these buildings produced much the same pressure pattern near the upwind corner of their rooftops for low parapets (the worst case). Figure 3 shows two of the pressure patterns. As explained in Refs. 1, 2 and 3 the pressure pattern plays a crucial role in the failure of certain types of roofing systems. The pressure pattern of course depends on the wind flow pattern; therefore a test rig can be considered satisfactory if it produces a pressure pattern reasonably similar to that in Figure 3. If the pressure pattern is satisfactory it can be safely assumed that the wind flow pattern is also realistic so that valid test results can also be obtained for gravel scour, membrane behaviour, etc. In other words, the test should be valid for virtually any type of roofing system.

The dimension "A" in Figure 3 has a value of about 25 ft. for the building sizes of the Figure. "A" is a measure of the size of the pressure pattern and is taken as the length of the -1.5 pressure coefficient contour. "A" would be proportional to building size, for a given shape; for

example, if the dimensions of, say, the high rise building were doubled, "A" for the new building would be 50 ft. There is thus some question as to what value should be adopted for "A" when designing the test rig, but the value of 25 ft can be considered reasonably representative. The roofing system sample should have dimensions of about 2.5A x 2.5A so that it at least covers the region where the pressure is substantially different from ambient ( $|C_p| > 0.5$ ). Preferably the sample should be even larger so that there are no spurious mechanical constraints in the critical portion of the sample (i.e. that portion of the sample exposed to the pressure pattern).

Since the sample size is directly related to the dimension "A" of Figure 3, equation (1.1) can be re-written and the objective of the present study can be summarized as follows: find the test-rig configuration which gives a pressure pattern like that in Figure 3 and for which the ratio

$$R_2 = \frac{\text{cross section area of jet of wind}}{A} \quad (1.2)$$

is minimum.

CHAPTER 3  
Apparatus and Test Procedures

3. Apparatus and Test Procedures

An apparatus was specially designed for this study. It consists of two main components:

- (a) a wind generator, and
- (b) a test platform

The wind generator had to be capable of producing a jet of wind whose cross-section dimensions could be easily varied. It consisted of an axial-flow fan, diffuser ducting with flow conditioning devices to ensure reasonably uniform flow, and a nozzle with adjustable flaps. The flaps allowed the cross-section dimensions of the jet of wind to be varied. The test platform consisted of a sheet of Plexiglass fitted with 53 static pressure taps. These enabled measurement of the pressure patterns produced when the jet of wind was directed at the platform. Figures 4a and 4b are schematic diagrams of the apparatus; photographs appear in Figures 5, 6 and 7. The wind generator is quite different from the aircraft engine/propeller arrangement (Figure 2) that would most probably be used to generate the jet of wind in the actual roofing system test rig. In the actual rig there will be no need to vary the cross-section dimensions of the jet of wind.

It is important that the flow in the jet of wind be reasonably uniform and free of swirl. Figure 8 shows velocity profiles measured with the largest jet cross-section dimensions. Away from the edges of the jet the velocity is constant within  $\pm 7\%$  which is quite acceptable. The uniformity is even better for smaller jet cross-sections because

there is then a greater static pressure drop across the nozzle; static pressure drops result in better flow uniformity in general. A substantial development effort was required to achieve the good flow quality evident in Figure 8. The flow straightener and mesh screens shown in Figure 4a were required to achieve this.

The experiments of the present study were carried out at reduced scale. The test platform seen in Figures 4b, 5 and 6 was 9 inches square. The results can be readily scaled up for whatever test-platform size is chosen for the actual test rig. This choice depends on what value is chosen for the full-scale dimension "A" of Figure 3. The discussion of Section 2 suggests a value of about 25 ft for "A" and a platform size of about 50 ft x 50 ft.

The wind generator produced a jet velocity of about 65 ft/sec. Since all pressure results are reduced to the form of non-dimensional pressure coefficients, they apply for any wind speed. Thus the pressure-coefficient results would apply directly for the full-scale test rig for all wind speeds.

The above discussion about scaling of the model results assumes that the Reynolds number was sufficiently high in the model tests. The Reynolds number, based on the dimension A, was of order 120,000 which is certainly high enough.

Ten basic test-platform configurations were investigated. These are listed in Table 1. Each basic configuration was tested with a range of wind-jet cross-section dimensions.

The test procedure consisted of setting up any particular configuration, running the apparatus and recording the pressures at each of the 53 taps on the test platform. The upstream corner of the test platform was always 8 3/4 inches from the end of the nozzle, as shown in Figure 4b. The jet of wind was fully contracted at this position for even the smallest nozzle opening size. A pitot tube at test-platform level was used to measure the dynamic pressure of the flow approaching the platform in each run.

All pressures were measured using water-filled manometer banks, with tubes inclined at 30 degrees to the horizontal for improved accuracy.

The pressure data were reduced to coefficient form and contour-plotted with the help of a computer program written for the purpose.



er height above the ground plane, in order to get a stronger up-wash flow up the walls of the platform. This was expected to produce stronger vortices (like those in Figure 1) and thus more-negative pressure coefficients. This configuration (vi) did indeed give improved Cp values but the improvement was small. As seen in Figure 10, the minimum pressure coefficients are only about -2.6, in comparison with about -3.5 in Figure 3. This is acceptable, but not particularly desirable since it would imply a need for a correction factor of  $\sqrt{2.6/3.5} = 0.85$  for the wind speed. That is, a wind speed of 100 mph in the test rig would produce the same actual suction (in psf) as an actual wind of only 85 mph. It proved impossible to get significantly higher suction (more negative Cp's) with an open-jet configuration. This is not surprising: the actual wind cross section is, in effect, infinitely large compared to the size of a building but this is not true in the test rig. Interference effects are therefore substantial and it is well known [6] that for open-jets the interference effects are such as to reduce suction pressures.

The jet cross-section dimensions of Figure 10 are the minimum values for which reasonably satisfactory results could be obtained for configuration (vi). Reducing the dimensions below the quoted values led to a fairly abrupt reduction in suction pressures. On the other hand, increased jet dimensions gave virtually the same peak suction coefficients and only slightly larger values of the dimension "A". This trend is illustrated by comparison of Figures 11 (small jet) and 12 (large jet) with Figure 10. Other configurations produced a similar trend as jet size was varied.

Configuration (viiia) was the same as configuration (vi) except that the  $6^{\circ}$  vortex generators were replaced by 1/4 inch high parapets. This configuration was inferior to configuration (vi): the minimum  $C_p$  value was only -2.0 for configuration (viiia). Figure 13 shows the results.

With an open jet the most effective test platform configuration was in fact the simplest, namely the plain test platform with no vortex generators or parapets. This configuration (viib), gave the results shown in Figure 14.

#### 4.2 Enclosed Jet Configurations

Interference effects with solid boundaries tend to be in the opposite sense to those for open jets. This led us to try configuration viii (Table 1), which would use an enclosure around the test platform, as sketched in Figure 15. The apparatus was set up as in Figures 15 and 16 for the model studies of enclosed jet configurations. This did not in fact give more negative  $C_p$ 's but it is nevertheless a promising configuration since the wind jet cross section can be smaller than for open jet configurations.

As for the open jet case, the pressure contour patterns were insensitive to the jet cross-section size until this was reduced below some minimum size; further reduction of jet size resulted in progressive deterioration of the pressure pattern. The optimum enclosure dimensions were found to be 8 3/4 in. wide by 7 in. high, with a 1 3/4 in. high test platform. The results for configurations (viiiia) and (viib) are shown in Figures 17 and 18, respectively, for the optimum enclosure cross section dimensions.

It should be noted that the pressure coefficients for the enclosed-jet cases are based on the wind dynamic pressure at the enclosure exit, (i.e. at station 2 in Figure 16). The static pressure at this station is generally quite close to atmospheric pressure; therefore pressure coefficients, jet cross-section dimensions and jet velocities based on conditions at station 2 can be directly compared with results for the open jet configurations. The jet heights given in Figures 17, 18 and 21 are the distances from the ceiling of the enclosure to the top of the test platform.

As seen by comparing Figures 17 and 18, configuration (viiiia), which has  $\beta = 6^\circ$  vortex generators attached to the upstream edges of the test platform, is best. Other configurations were also tested in an enclosed jet but configurations (viiiia) and (viiiib) gave superior results and only these two configurations were tested in detail for a range of enclosure cross-section sizes.

As mentioned in Chapter 2, the roofing system sample should have dimensions of at least  $2.5A \times 2.5A$ . Therefore the test platform would extend beyond the sides of the enclosure, as sketched in Figure 15. Some form of flexible seal would be required where the lower edges of the enclosure side walls meet the test platform. This would be necessary to avoid spurious mechanical constraints on the roofing system sample.

#### 4.3 Configurations With A Divider Plate

As mentioned in Chapter 2, the critical wind direction is at  $45^\circ$  to the upstream walls of a building and the test

rig would simulate this condition. Therefore the flow pattern over the test platform would be symmetrical about a vertical plane of symmetry passing through the diagonal of the test platform. Moreover, previous 1:10 scale wind tunnel tests of buildings with various roofing systems installed have shown that failure generally initiates to the sides of the plane of symmetry [1, 2, 4, 5, 7 and 8]. That is, the failure process does not "cut across" the plane of symmetry. It should therefore be adequate to simulate wind conditions on only one side of the plane of symmetry, with still air on the other side. This would allow halving of the jet cross-section with a corresponding reduction of wind-generator size and power. This would imply a substantially lower rig cost.

To implement this scheme a vertical divider panel would be used. This panel would coincide with the plane of symmetry and would have to extend at least 1.5 platform heights upstream of the upwind corner of the test platform. This approach could be used with both open and enclosed jet configurations. This panel would extend to the top of the enclosure, or a little above the upper boundary of open jets. The roofing system sample would still be installed over the entire test platform. As with enclosure sidewalls, some form of flexible seal would be required where the divider panel meets the test platform surface. The general arrangement is sketched in Figure 19. In the case of an enclosed jet, the divider panel would simply become one sidewall of the enclosure.

The best open jet and enclosed jet configurations (corresponding to Figures 14 and 17 respectively) were re-tested with a divider panel installed on the model. The

results are shown in Figures 20 and 21; comparison with Figures 14 and 17, respectively, shows that the results with a divider panel are very similar to those without. This indicates that use of a divider panel is indeed acceptable. The recommended configurations, those of Figures 20 and 21, therefore incorporate divider panels.

CHAPTER 5  
Recommendations and Cost Estimates

5. Recommendations and Cost Estimate

Both an open jet and a closed jet configuration are recommended initially. Clearly there must be a compromise between cost and rig size and maximum wind speed capability. The information is presented in such a way that SPRI can choose the compromise which is most compatible with its constraints.

5.1 Recommended Open Jet Configuration

As already mentioned, the configuration corresponding to Figure 20 represents the optimum for the open jet case. Particulars are as follows:

- plain platform, height above ground plane,  
     $H = 1.04A$ , with divider panel
- jet width,  $w = 1.35A$  (5.1)
- jet height,  $h = 1.8A$
- maximum suction pressure coefficient,  $C_{p_m} = -2.7$

where "A" is a measure of the size of the pressure pattern as discussed in Chapter 2.

Since the maximum suction coefficient is less negative than the desirable value of -3.5, the test rig would have to produce a higher wind speed,  $V$ , to simulate an actual wind speed,  $V_w$ , at roof level. As mentioned in Section 4.1, this is necessary to produce about the same variation of actual pressure over the test sample as the real wind would produce on a building rooftop. In this case the relation between  $V$  and  $V_w$  is  $V = \sqrt{3.5/2.7}$  or  $V_w = 1.14 V$ .

The power required to produce a jet is given by the following expression:

$$\begin{aligned}\text{Power} &= \text{Kinetic Energy Flux}/\eta \\ &= (\text{mass flow rate}) \times \frac{v^2}{2}/\eta \\ &= \rho \times \text{jet area} \times v \times \frac{v^2}{2}/\eta\end{aligned}$$

where -  $\eta$  is a fan or propeller efficiency and would have a value of about 0.8

-  $\rho$  is the density of atmospheric air at sea level

For the optimum open jet configuration the expression for power becomes:

$$\begin{aligned}P &= \rho \times 1.35A \times 1.8A \times 1.14V_w \times \frac{(1.14V_w)^2}{2} \times \frac{1}{0.8} \quad (5.2) \\ P &= 2.25 \rho A^2 V_w^3\end{aligned}$$

## 5.2 Recommended Enclosed Jet Configuration

As already mentioned, the configuration corresponding to Figure 21 represents the optimum for the enclosed jet case. Particulars are as follows:



- platform with  $\beta = 6^\circ$  vortex generators, height above ground plane,  $H = 0.64 A$ , with divider panel.
- enclosed jet width,  $w = 1.6A$
- enclosed jet height,  $h = 1.9A$  (5.3)  
(at station 2, Figure 16)
- maximum suction pressure coefficient,  $C_{p_m} = -2$
- $V = \sqrt{3.5/2.0} V_w = 1.33 V_w$

As in Section 5.1, the power can be estimated at:

$$P = \rho \times 1.6A \times 1.9A \times 1.33V_w \times \frac{(1.33V_w)^2}{2} \times \frac{1}{0.8} \quad (5.4)$$
$$P = 4.47 \rho A V_w^3$$

From eq (5.2) it is clear that the enclosed jet configuration would require about twice as much power as the open jet configuration for the same pressure pattern size,  $A$ , and the same wind speed,  $V_w$ . Moreover the enclosed jet would have to be larger than the open jet ( $1.6A \times 1.9A$  versus  $1.35A \times 1.8A$ ). Therefore it is clear at this point that the enclosed jet configuration is relatively unattractive and it will not be considered further. The main reason for its unattractiveness is that the size of pressure pattern produced by the optimum enclosed jet configuration is substantially less than that of the optimum open jet configuration (compare Figures 20 and 21).

### 5.3 Cost Estimate for Recommended Open Jet Configuration

Since the open jet configuration has been shown to be substantially more attractive, cost estimates are provided for it only. The optimum configuration (ix of Table 1) is summarized in Section 5.1. For given choices of contour pattern size,  $A$ , and wind speed,  $V_w$ , equation (5.2) can be used to estimate the power required for the test rig and equation (5.1) determines the cross-section dimensions required for the jet.

As discussed in Chapter 2, 25 feet would be a reasonably representative value to choose for "A". The test rig should be capable of simulating wind speed,  $V_w$ , equal to the speed of the strongest one-second gusts which the roofing system is required to withstand.

Tables 2a, 2b and 2c give power and cost estimates for a range of wind speeds,  $V_w$ , and pressure pattern size parameter,  $A$ , equal to 10, 17 and 25 feet respectively. The power estimates are from equation (5.2). The Appendix gives a breakdown of the cost estimates for some of the cases of Table 2 so that some appreciation can be gained of the major contributing cost items.

In view of the very large powers required, large aircraft gas turbine engines (turboprop engines) are the most attractive power source. The only possible alternative would be very large electric motors which would have to be custom built and would be very expensive (in the million dollar range). Moreover electric motors would be very large in size, which would necessitate a long shaft between the motor and the propeller; substantial engineering design costs would be incurred in designing the motor/propeller drive and bearing system. All this is avoided by using an aircraft turboprop engine/propeller unit. Moreover, there is a good possibility that used aircraft engine/propeller units can be procured at a fraction of the price of new units.

There is only one suitable turboprop engine/propeller unit available: the Allison T-56 which propels the Lockheed Hercules transport aircraft. Other units are either too small (e.g. Rolls-Royce Dart, Pratt & Whitney PW-100 series) or were not used in sufficiently large numbers to be reasonably available on the second-hand market (e.g. Rolls-Royce Tyne; Bristol-Siddeley Proteus). The T-56 Hercules unit drives a 13 1/2 ft. diameter propeller and delivers a maximum of 4000 to 5000 HP. It is thus quite suitable for present purposes. Earlier versions of the engine deliver about 4000 HP; later versions, about 5000. In the present application it would be desirable to run the engines at somewhat less than their maximum rating. The Hercules is a very widely used aircraft. Moreover there is a program in place under which the U.S. military plans to re-engine its Hercules aircraft with a new engine type. Many T-56 units would then be available at military-surplus prices. We have used an estimate of \$100,000 U.S. per engine/propeller unit. A new unit would cost about \$1,000,000 U.S.

Assuming that used engines are available at about \$100,000 per unit, the engine/propeller cost would only be a small part of the overall cost of a test rig. The engine fuel system and control console would in fact cost more than the engine itself! The engine mount system would have to be carefully engineered and would also be quite costly.

The optimum jet cross section is rectangular, its height being 1.33 times its width. Therefore there would have to be a substantial duct enclosing the propeller(s), and this duct would have to incorporate a transition of shape so that the final jet of wind has the required rectangular shape and dimensions. One or more engines/propellers could be used. In fact for most of the cases of Table 2 multiple engine/propeller units would be required to meet the power and/or size needs. Unfortunately the possibility of complex dynamic effects increases as the number of engine/propeller units increases and engineering-design and commissioning costs mount rapidly. The ducting would be quite massive for the larger installations and would have a fairly complex shape. The ducting is a major cost item.

Realistically, cases which would require more than 4, or perhaps 5, engine/propeller units should not be considered. The complexity and technical risk of such a rig would be excessive.

It is interesting to compare the cost estimates of Table 2 with figures for electricity generating plants. A rule for such plants is \$275 US per installed Horsepower of capacity. Assuming half of that is for the generators, etc., we are left with \$137 US per installed Horsepower for prime movers.

Estimates using this rule of thumb are in rough agreement with those of Table 2.

It is emphasized that the cost estimates of Table 2 are preliminary. They are sufficiently accurate to serve as a basis for selecting rig size and maximum wind speed. More detailed estimates could be obtained once a decision is made.

CHAPTER 6  
Discussion

6. Discussion

Although 25 ft is considered a representative value to use for "A", as discussed in Chapter 2, Table 2C shows that power and cost requirements are rather prohibitive for this choice. A value as small as 10 ft for "A" would most probably give misleading results for many roofing systems. For example, if we have a system which incorporates rigid boards or slabs whose maximum dimensions are about 4 ft., only three or four boards of any given row would be immersed in the jet of wind if A is chosen at 10 ft. Choosing 'A' equal to about 17 feet would probably be acceptable. The test rig would then produce pressure patterns similar to those at the upwind corner of the roof of a 10 ft. high low-rise building, or a 20 ft wide high rise building and results should be valid for roofing systems whose largest elements are no larger than 4 feet. However, Table 2b shows very high power requirements and cost estimates if the required wind speed exceeds about 100 mph. Clearly there are no easy choices!

An alternative that might be considered is that of renting time in an existing large wind tunnel rather than designing and building a special purpose wind generator. For example a 30 ft x 30 ft wind tunnel is available in Ottawa and can be rented from the National Research Council of Canada at about \$500 US per hour. The tunnel is capable of speeds  $V_1$  up to 120 mph in the test section when a low-drag model is installed. A test platform corresponding to the optimum enclosed jet configuration of Figures 17 and 21 could be placed in this tunnel. The tunnel height of 30 ft would, in this case, be the limiting dimension and would restrict

the platform height to 7.5 ft., leaving a 22.5 ft. high jet of wind above the platform. The pressure-pattern size parameter,  $A$ , would have a value of 12 ft. Unfortunately this is a rather low value. Furthermore, the test platform would produce a very high drag and would seriously reduce the maximum speed capability of the tunnel. Recall that for the enclosed jet configuration the speed of the test wind must be larger than that of the actual wind,  $V_w$ , by a factor of 1.33 (see Section 5.2). Thus this alternative is not very attractive but SPRI may wish to give it serious consideration in view of the high costs of a special purpose test rig.

If SPRI chooses a special purpose test rig, cost considerations will most probably dictate selecting pressure pattern size and jet velocity a good deal smaller than would ideally be desired - say  $A = 15$  ft. and  $V_w = 100$  mph; requiring about 6900 HP and two T-56 engine/propeller units, with an estimated cost of \$1,450,000 US.



CHAPTER 7  
Conclusions

7. Conclusions

An experimental study has been carried out to determine the optimum test-rig configuration for assessing the resistance of full-size samples of roofing systems to damage by high winds. The study was carried out at reduced scale.

A variety of open jet and enclosed jet configurations were investigated. An open jet configuration has been identified as the optimum. Unfortunately, even for the optimum configuration power requirements and costs would be very high if ideally desirable pressure pattern size and maximum wind speed were to be chosen. Some compromise will probably be necessary.

References

References

1. Kind, R.J. and Wardlaw, R.L.  
"Failure Mechanisms of Loose-laid Roof Insulation Systems"  
Journal of Wind Engineering and Industrial Aerodynamics, Vol. 9, 1982, pp. 325-341
2. Kind, R.J. and Wardlaw, R.L.  
"Wind Tunnel Tests on Loose-Laid Roofing Systems for Flat Roofs"  
Proceedings of Second International Symposium on Roofing Technology  
Sept. 1985, pp. 230-235
3. Kind, R.J.  
"Proposal for an Engineering Study to Define Equipment for Full-Scale Testing of Wind Resistance of Loose-Laid Roofing Systems"  
GastOPS Ltd. Report GTL-52-1-P.1  
September 1986
4. Kind, R.J., Savage, M.G., Wardlaw, R.L.  
"Further Model Studies of the Wind Resistance of Two Loose-Laid Roof Insulation Systems (High Rise Buildings)"  
National Research Council of Canada Report LTR-LA-269  
April 1984
5. Kind, R.J., Savage, M.G., Wardlaw, R.L.  
"Further Wind Tunnel Tests of Loose-Laid Roofing Systems"  
National Research Council of Canada Report LTR-LA-294  
March 1987
6. Pankhurst, R.C., Holder, D.W.  
Wind-Tunnel Technique  
Pitman, London, 1952
7. Kind, R.J.  
"Further Wind Tunnel Tests on Building Models to Measure Wind Speeds at Which Gravel is Blown off Rooftops"  
National Research Council of Canada Report LTR-LA-189  
August 1977
8. Kind R.J. and Wardlaw, R.L.  
"Model Studies of the Wind Resistance of Two Loose-Laid Roof-Insulation Systems"  
National Research Council of Canada Report LTR-LA-234  
May 1979

Tables

CHAPTER 4

Results

#### 4. Results

Some of the basic configurations of Table 1 yielded poor pressure distributions. In particular the minimum pressure coefficients were sometimes only of order -1.0 or even higher; from Figure 3 we see that minima of about -3.5 are desired. The areas over which the pressure coefficients differed from zero were also rather small. No results are presented for those configurations which did not show any promise.

##### 4.1 Open Jet Configurations

Configuration (i) showed initial promise, giving a good contour pattern with a minimum  $C_p$  value of -2.3. Figure 9 shows results for the optimum jet cross-section size. The next configuration which showed some promise was configuration (iii) with  $\beta = -6^\circ$  and  $\gamma = 90^\circ$ .  $\beta$  is a vortex-generator angle defined in Figure 2 and  $\gamma$  is  $90^\circ$  when the vortex generators are positioned at the leading edges of the test platform. The only value of  $\gamma$  which worked well was  $90^\circ$ . The higher values of  $\beta$  (i.e.  $\beta > 6^\circ$ ) also did not work well. With a moderate jet size and  $\beta = 6^\circ$ ,  $\gamma = 90^\circ$ , configuration (iii) gave a minimum  $C_p$  of -2.2 and a good overall contour pattern, that is a pattern similar to those of Figure 3. Configuration (iv) involved leaning the vortex generators over the test platform and it gave virtually the same results as configuration (iii). In configuration (v) the vortex generators were replaced by parapets; this too gave results very similar to those of configuration (iii). At this point in the test program, the test platform was raised to a great-

Table 1  
Test-Platform Configurations Investigated In Present Study

Configuration	Description (all dimensions are model scale)
i	plain 9" x 9" platform, 1 3/4" above ground plane
ii	9" x 9" platform flush with ground plane, vortex generators, $\beta = 6^\circ$ (see Figure 2) at platform leading edges
iii	9" x 9" platform, 1 3/4" above ground plane, vortex generators with $\beta = 6^\circ$ ; $20^\circ$ , $30^\circ$ and $45^\circ$ mounted at platform leading edges ( $\gamma = 90^\circ$ ) and also with $\gamma = 105^\circ$ , $120^\circ$
iv	9" x 9" platform, 1 3/4" above ground plane, vortex generators with $\beta = 6^\circ$ mounted at platform leading edges with vortex generators leaned inwards $10^\circ$ and $30^\circ$
v	9" x 9" platform, 1 3/4" above ground plane, with 1/4" high parapets at leading edges of platform
vi	9" x 9" platform, 3 5/8" above ground plane, with $\beta = 6^\circ$ vortex generators at platform leading edges
vii	9" x 9" platform, 3 5/8" above ground plane: (a) with 1/4" high parapets at platform leading edges (b) plain platform (i.e. parapets removed)
viii	enclosed jet with 9" x 9" platform, 1 3/4" above ground plane, (see Figure 14) (a) with $\beta = 6^\circ$ vortex generators at platform leading edges (b) plain platform (i.e. vortex generators removed)
ix	open jet with divider panel; 9" x 9" platform 3 5/8" above ground plane; plain platform
x	enclosed jet with divider panel; 9" x 9" platform, 1 3/4" above ground plane with $\beta = 6^\circ$ vortex generators at platform leading edges



Table 2

Estimated Power Requirements and Costs for Recommended Test-Rig Configuration (see Section 5.1 of text)

Table 2a - A = 10 ft; jet width = 13.5 ft; jet height = 18 ft; platform height = 10 ft.

Case	Maximum Wind Speed, $V_w$ (mph)	Power (horsepower)	Number of T-56 Units Required	Cost Estimates (US \$)
A	100	3046	1	\$ 672,000 *
B	125	5950	2	\$ 962,000 *
C	150	10280	3	\$ 1,276,000

Table 2b - A = 17 ft; jet width = 23 ft; jet height = 30.6 ft; platform height = 17.7 ft.

Case	Maximum Wind Speed, $V_w$ (mph)	Power (horsepower)	Number of T-56 Units Required	Cost Estimates (US \$)
D	100	8803	2	\$ 1,761,000
E	125	17193	4	\$ 2,434,000
F	150	29710	6 or 7	\$ 3,351,000

Table 2c - A = 25 ft; jet width = 33.8 ft; jet height = 45 ft; platform height = 26 ft.

Case	Maximum Wind Speed, $V_w$ (mph)	Power (horsepower)	Number of T-56 Units Required	Cost Estimates (US \$)
G	100	19040	5	\$ 6,027,000
H	125	37180	9	\$ 7,983,000
I	150	62250	15	\$11,117,000

\* see Appendix for breakdown

Figures

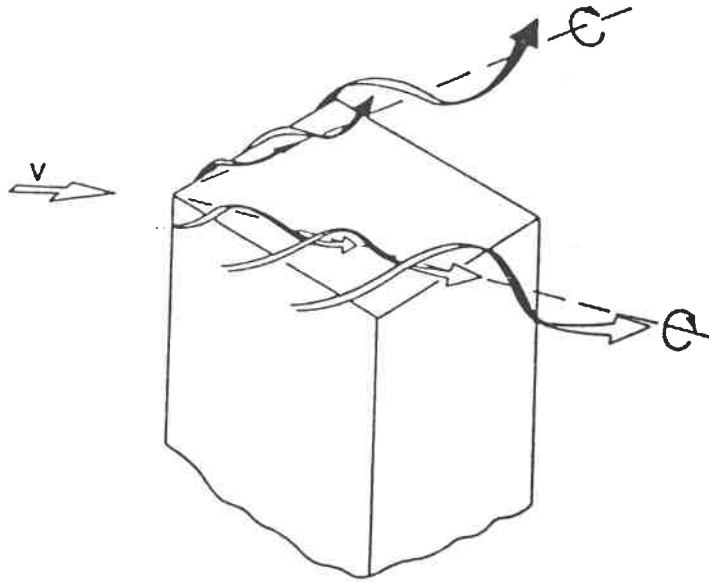


Figure 1 Sketch of Flow Over Rooftop for  
45° Wind Direction

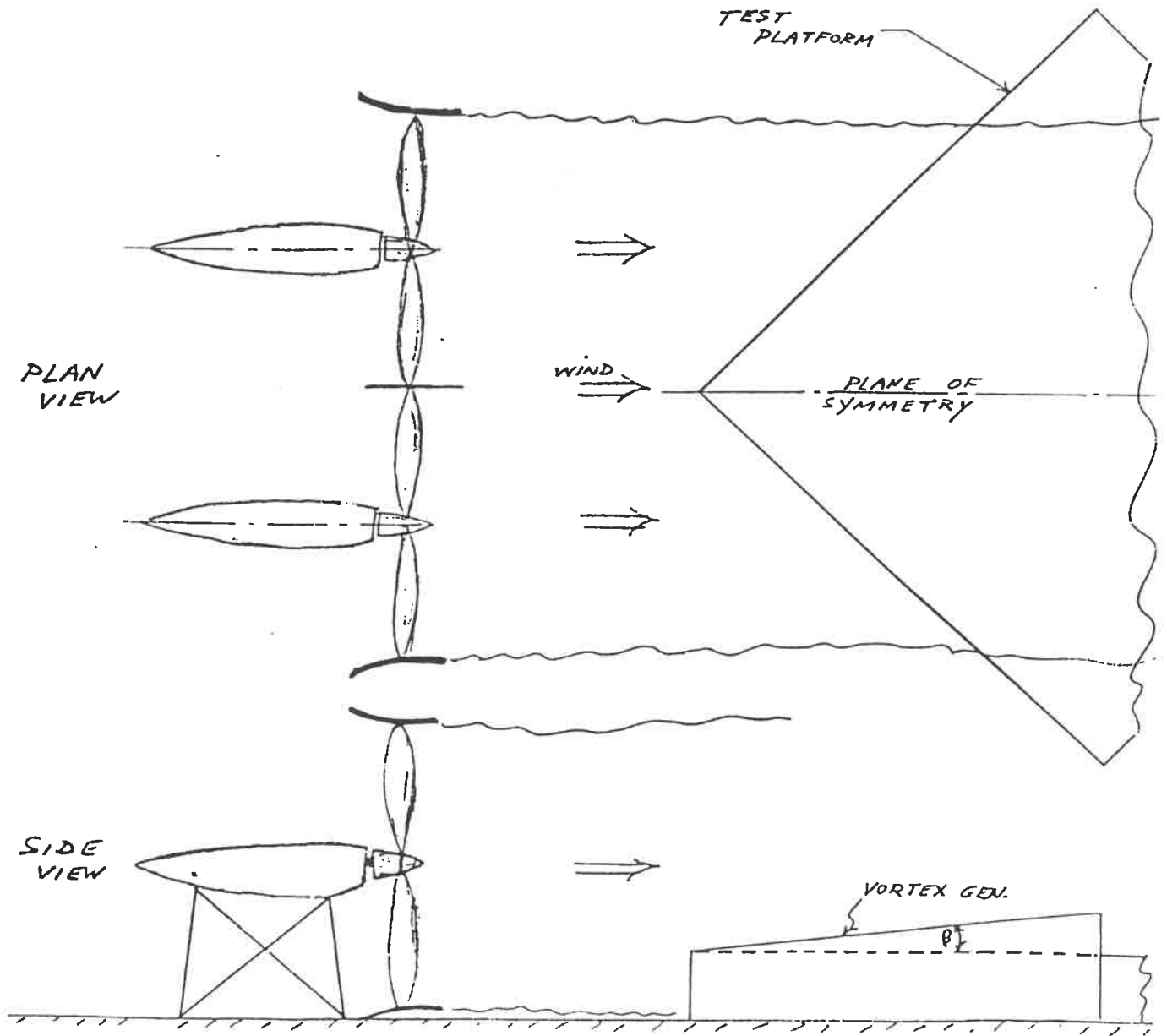
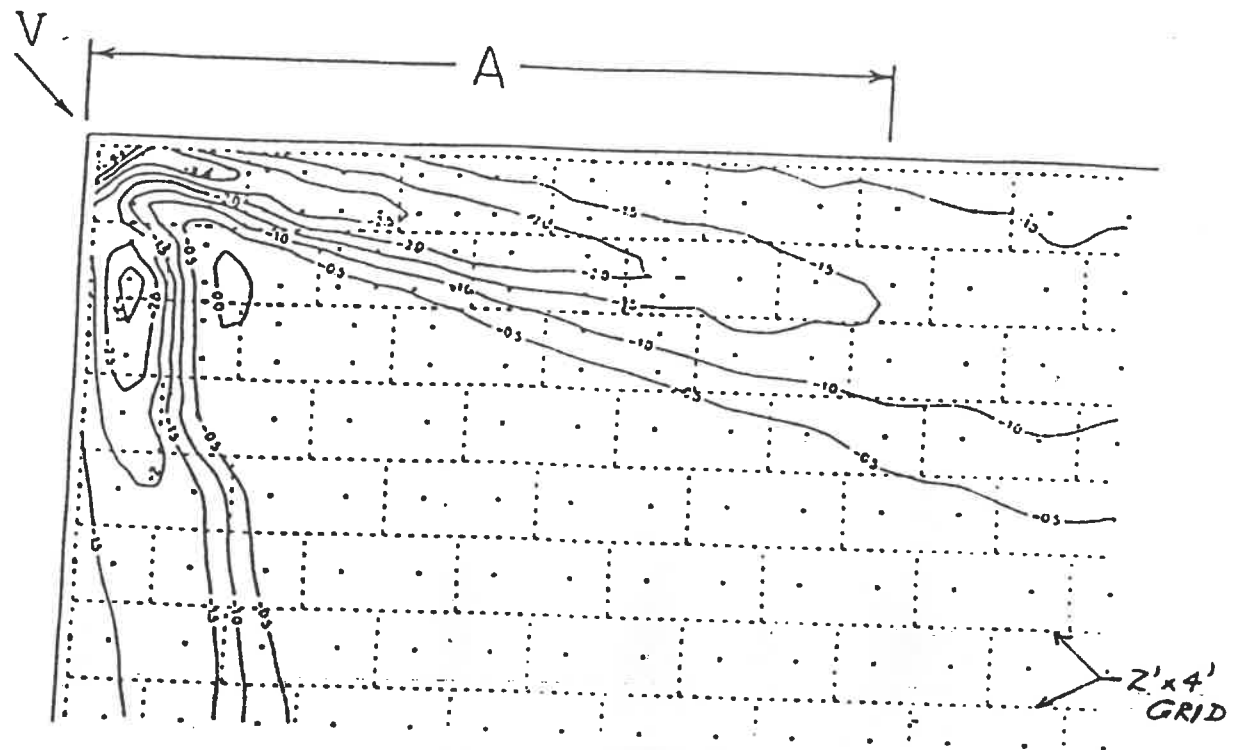
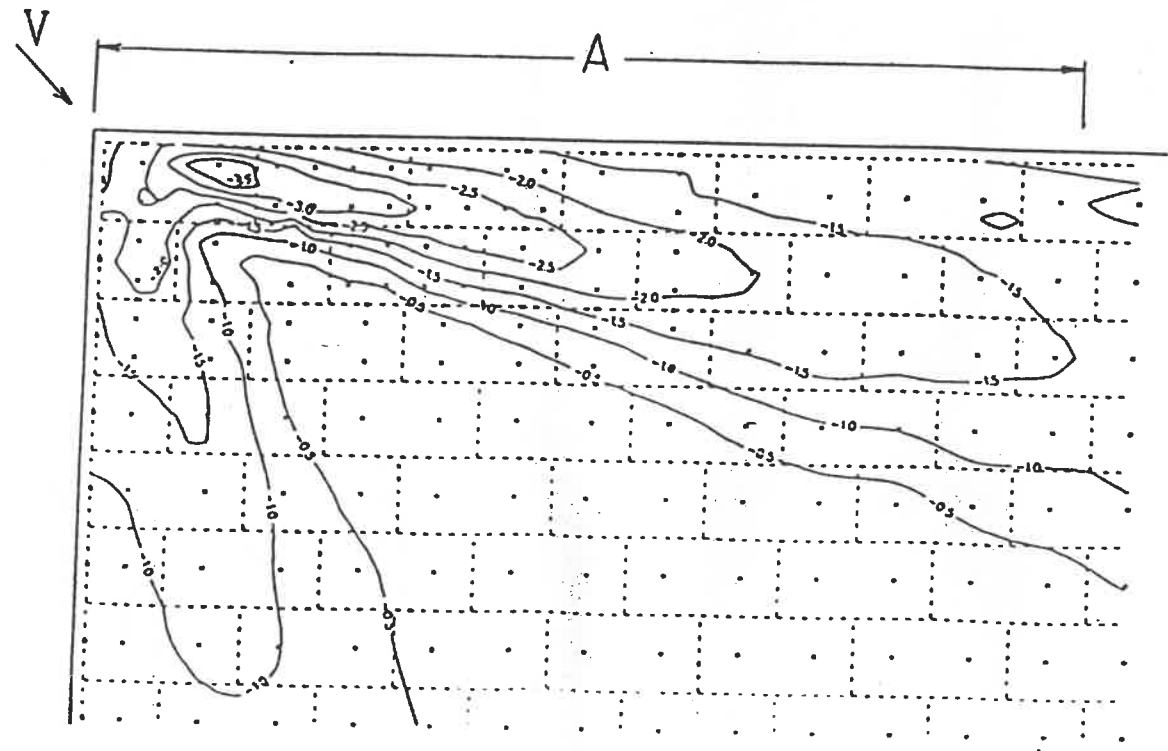


Figure 2 Schematic of Expected General Appearance of Test Rig

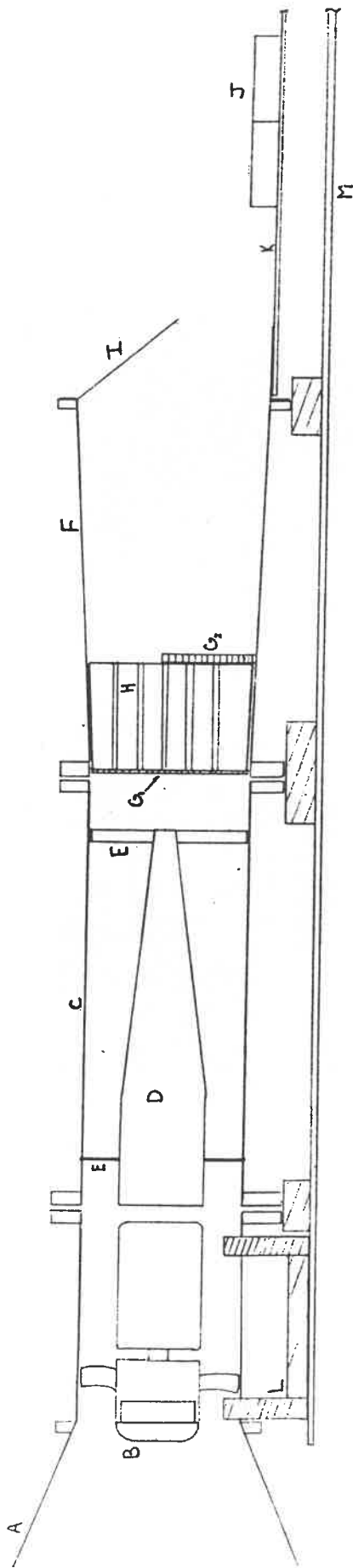


(a) 15' high x 77' long x 53' wide Low-Rise Building, parapet height = 0.7'



(b) 75' high x 60' long x 30' wide High-Rise Building, parapet height = 0.7'

Figure 3 Pressure Coefficient Contours Near Upwind Corner of Buildings for 45° Wind Direction (from Ref. 4)



- A = INLET CONE
- B = SPINNER
- C = FIRST DIFFUSER DUCT
- D = TAIL CONE
- E = TAIL CONE SUPPORT
- F = SECOND DIFFUSER DUCT
- G<sub>1</sub> = WIRE MESH SCREEN
- G<sub>2</sub> = WIRE MESH SCREEN (Double Layer)
- H = FLOW STRAIGHTENER
- I = NOZZLE FLAPS
- J = MODEL
- K = GROUND BOARD
- L = FAN CRADLE
- M = TABLE

SPRI TEST RIG  
ASSEMBLY  
 SCALE: 1/2" = 12"  
 Drawn by: 18

Figure 4a Schematic Diagram of Apparatus (Side View)

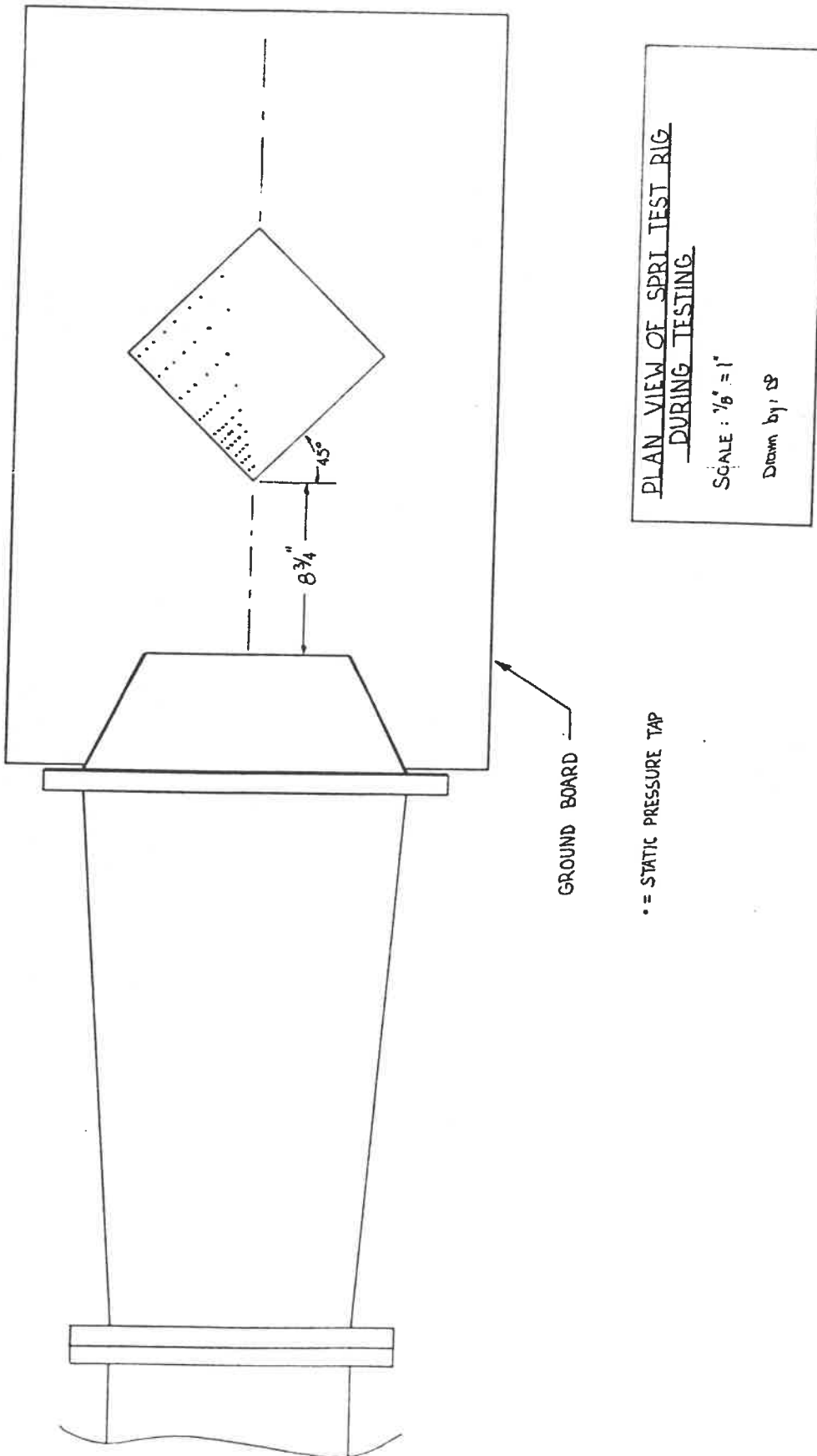


Figure 4b Schematic Diagram of Apparatus (Plan View of Downstream Portion)

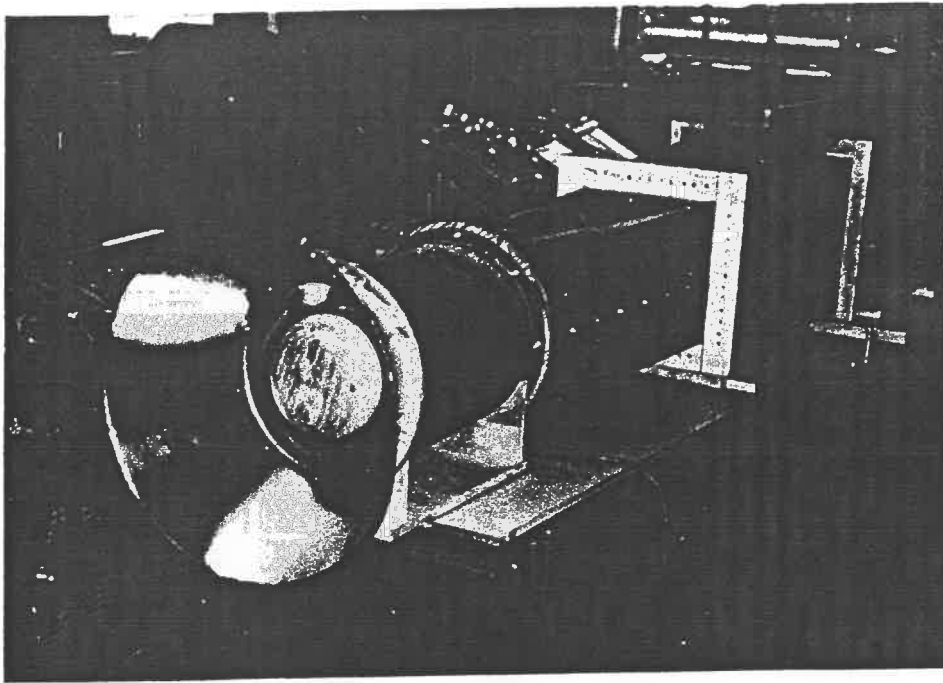


Figure 5 Photograph of Apparatus Used in Present Study  
(view of Intake End)

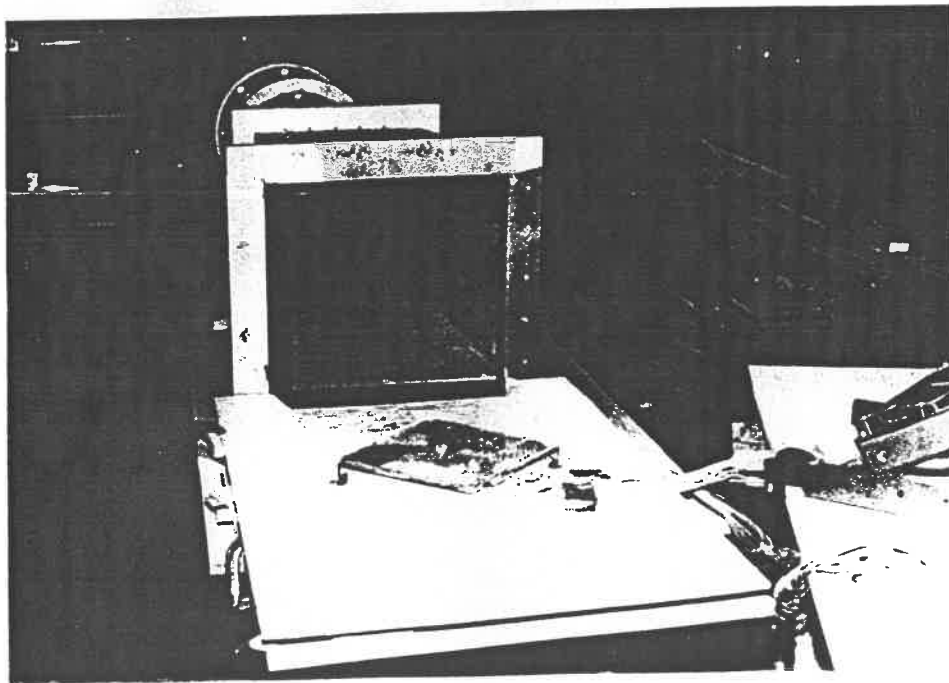


Figure 6 Photograph of Apparatus Used in Present Study  
(View of Nozzle End, Showing Ground Board and  
Test Platform)



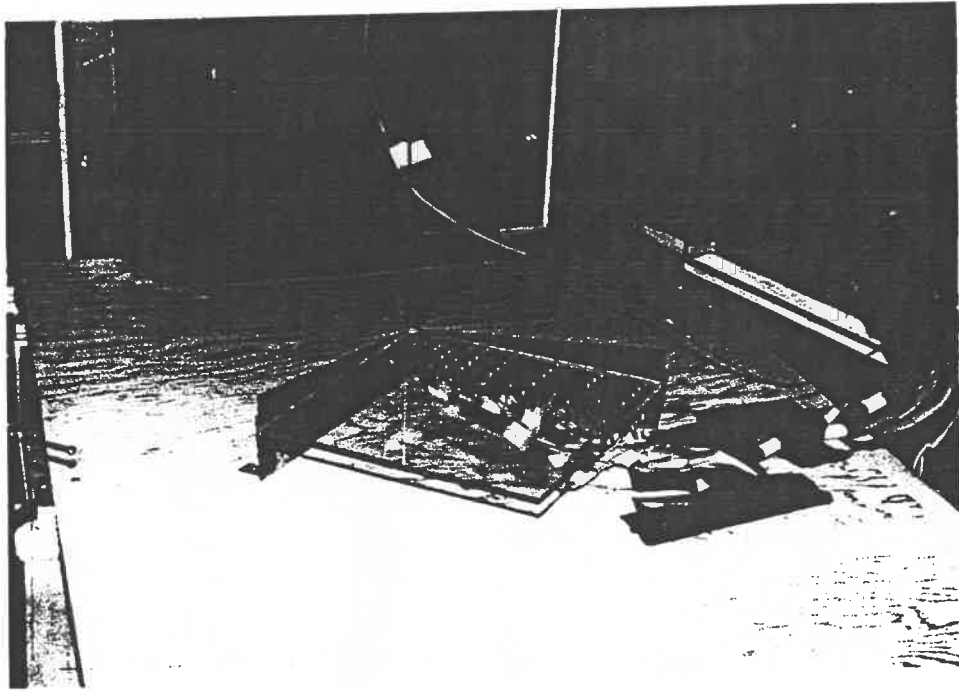


Figure 7 Photograph of Apparatus Used in Present Study  
(Close-up of Nozzle and Test Platform)

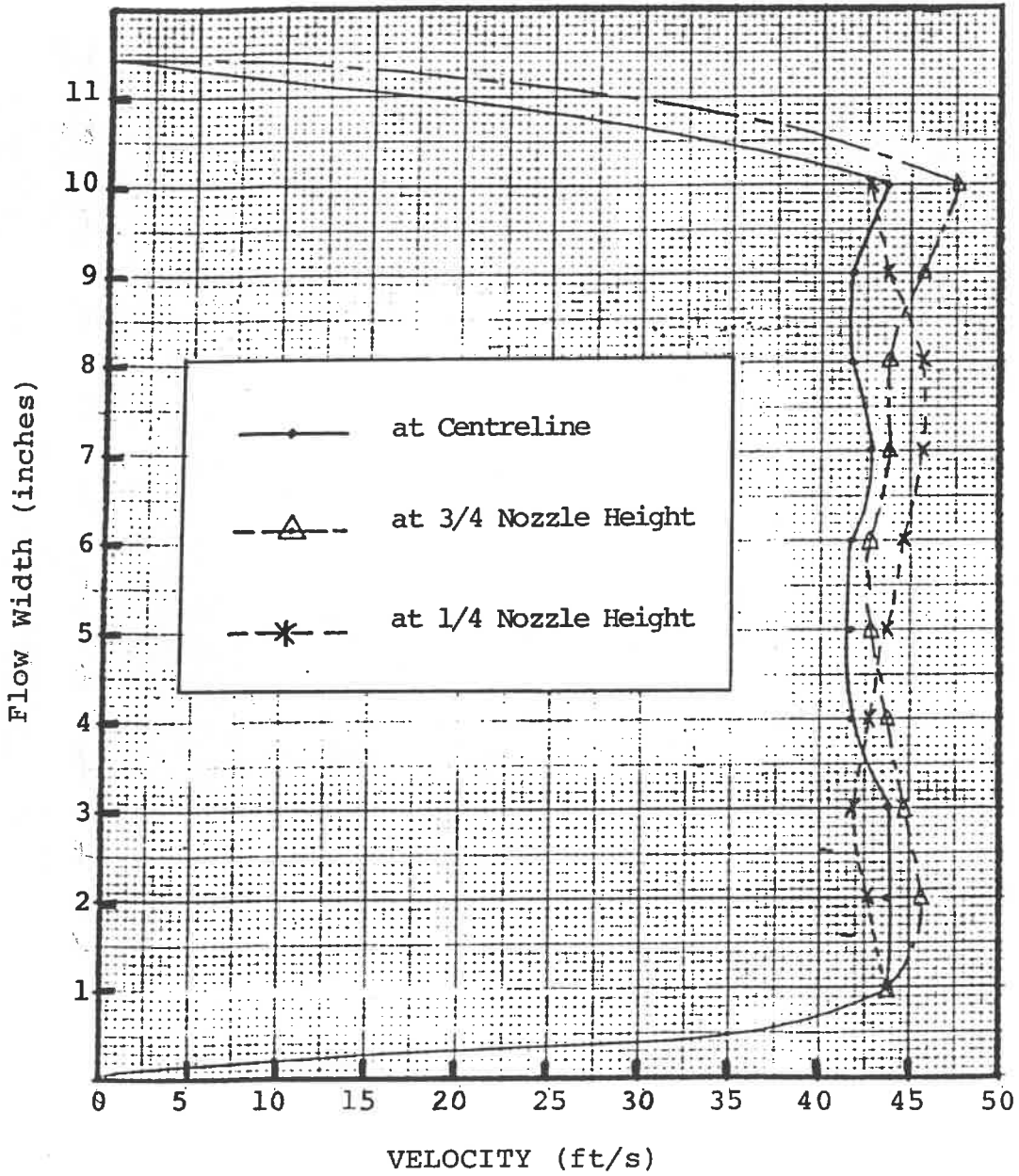


Figure 8 Velocity Profiles at Nozzle Exit for 11 1/2" wide x 11 5/8" high jet cross-section

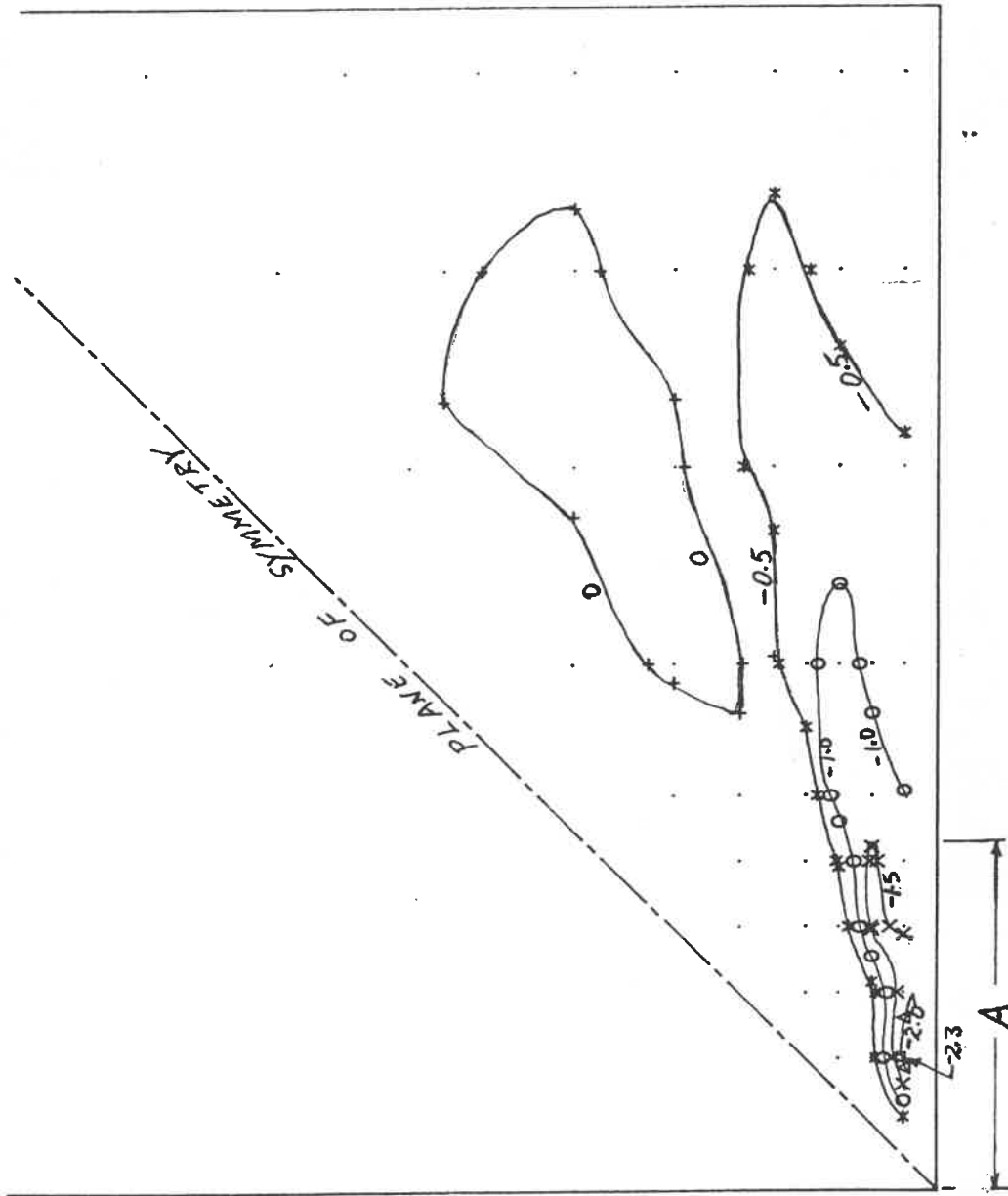


Figure 9 Pressure-Coefficient Contours Obtained with Configuration (i) for  
9 1/2 in. wide by 6 3/8 in. high (3.7A x 2.5A) Open Jet (Optimum  
Jet Dimensions)

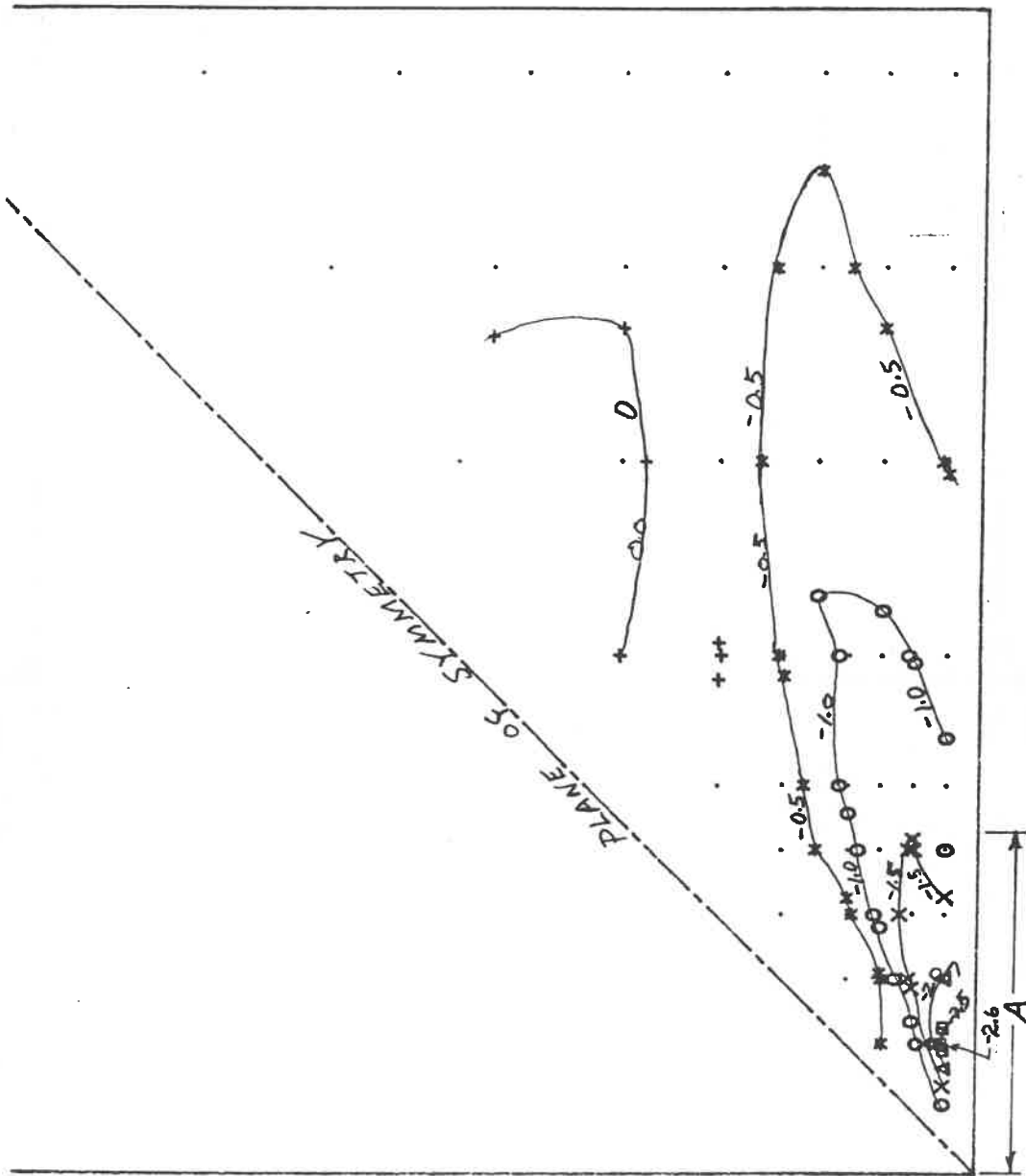


Figure 10 - Pressure Coefficient Contours for Configuration (vi) with  
9 1/2 in. wide by 6 3/8 in. high (3.4 A x 2.4A) Open Jet  
(Optimum Jet Dimensions)

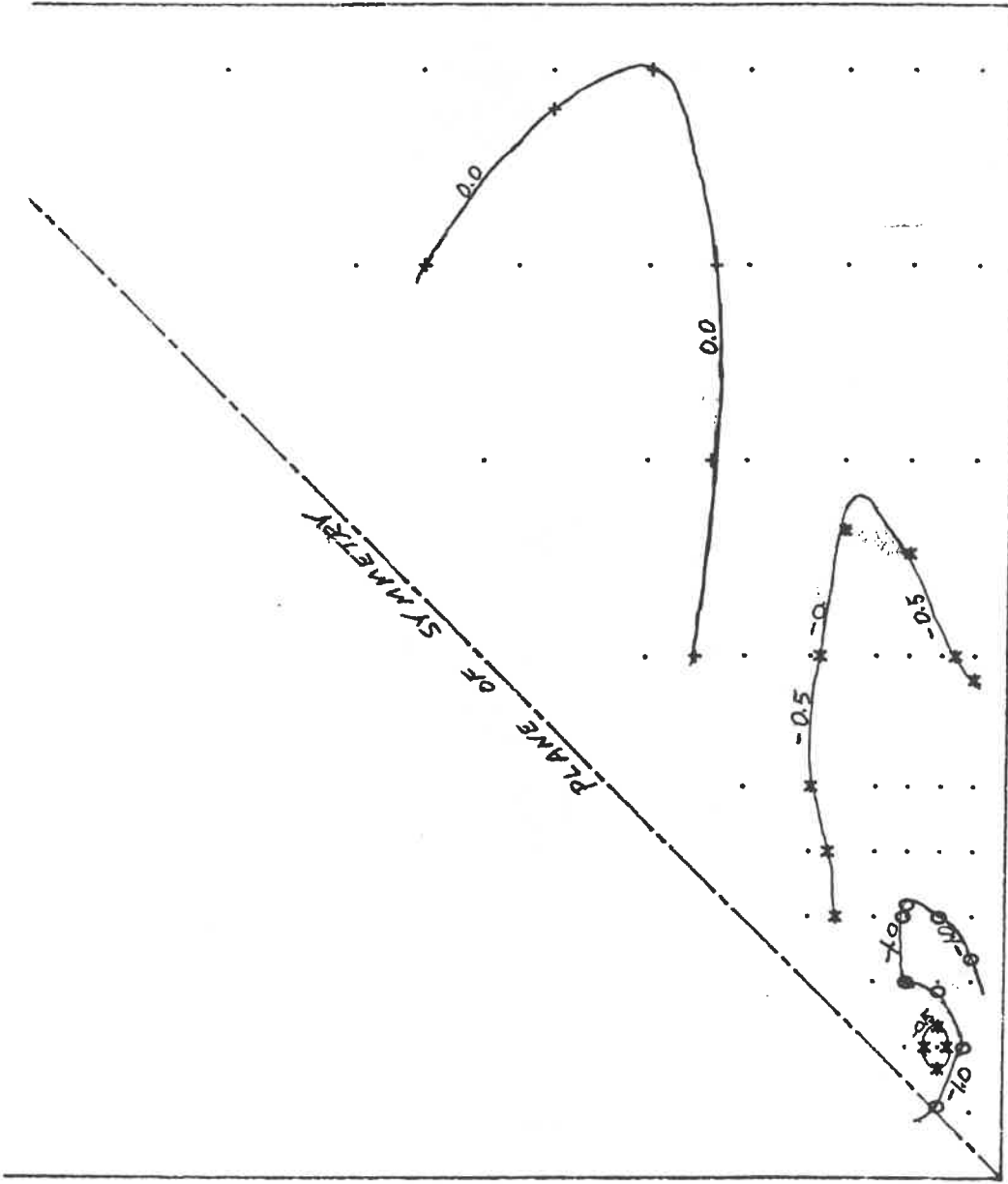


Figure 11 Pressure-Coefficient Contours for Configuration (vi) with  
7 1/2 in. wide by 5 in. high Open Jet (Jet too small)

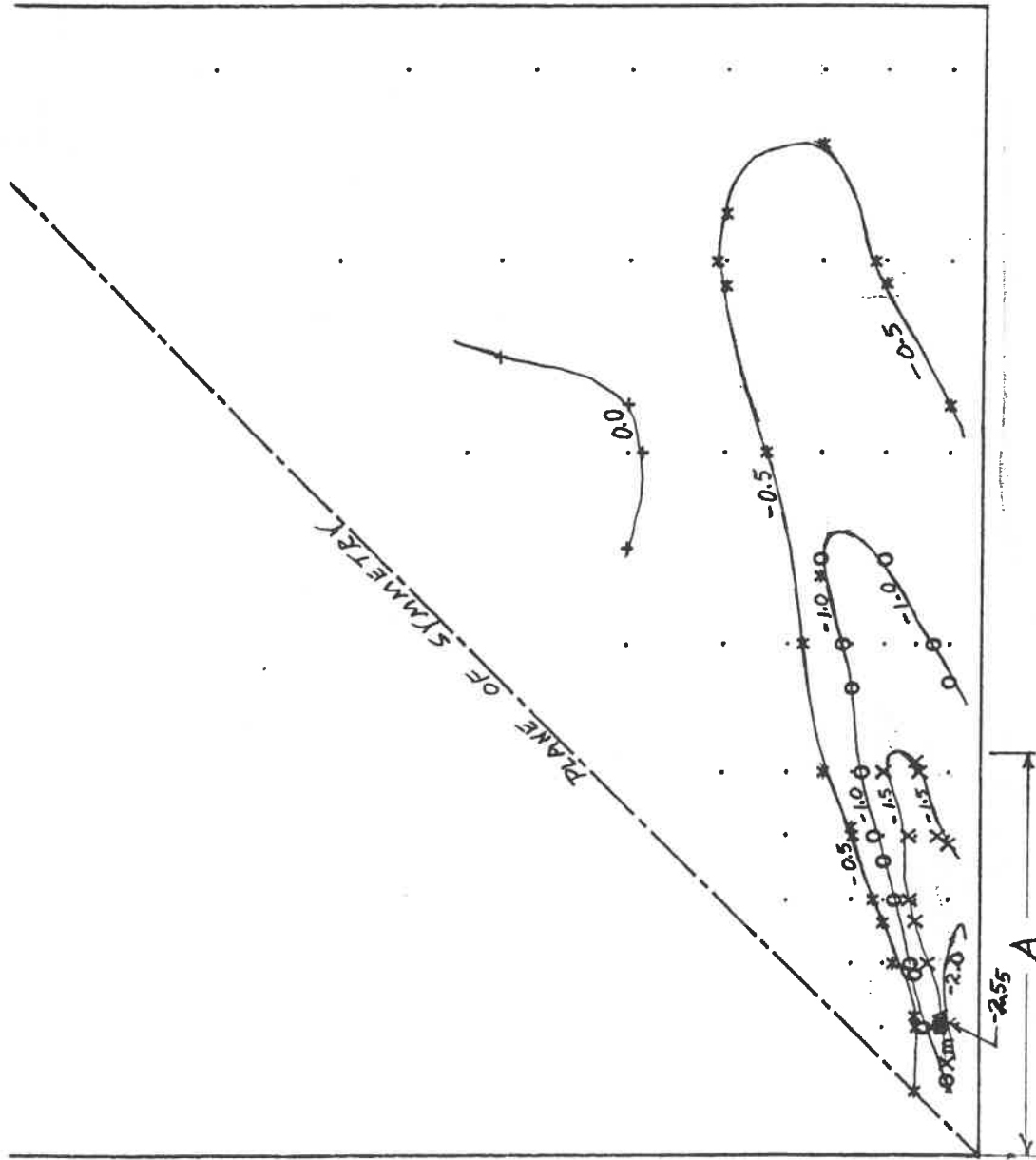


Figure 12 Pressure-Coefficient Contours for Configuration (vi) with 10 in. wide by 10 1/2 in. high (3.2A x 3.4A) Open Jet (Jet larger than optimum)

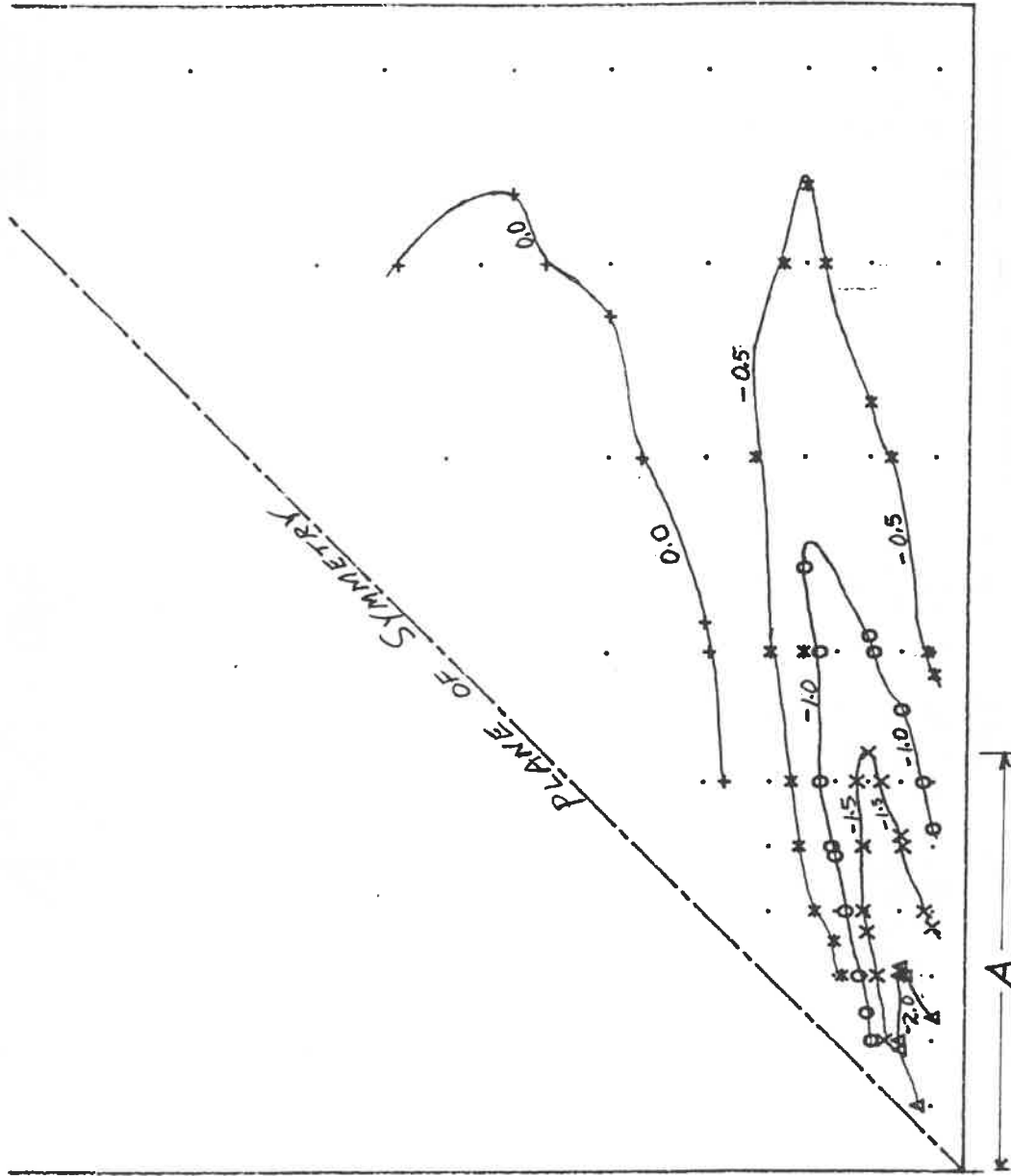


Figure 13 Pressure Coefficient Contours for Configuration (via) with 9 1/2 in. wide by 6 3/8 in. high (3.0A x 2.0A) Open Jet (Optimum Jet Size)

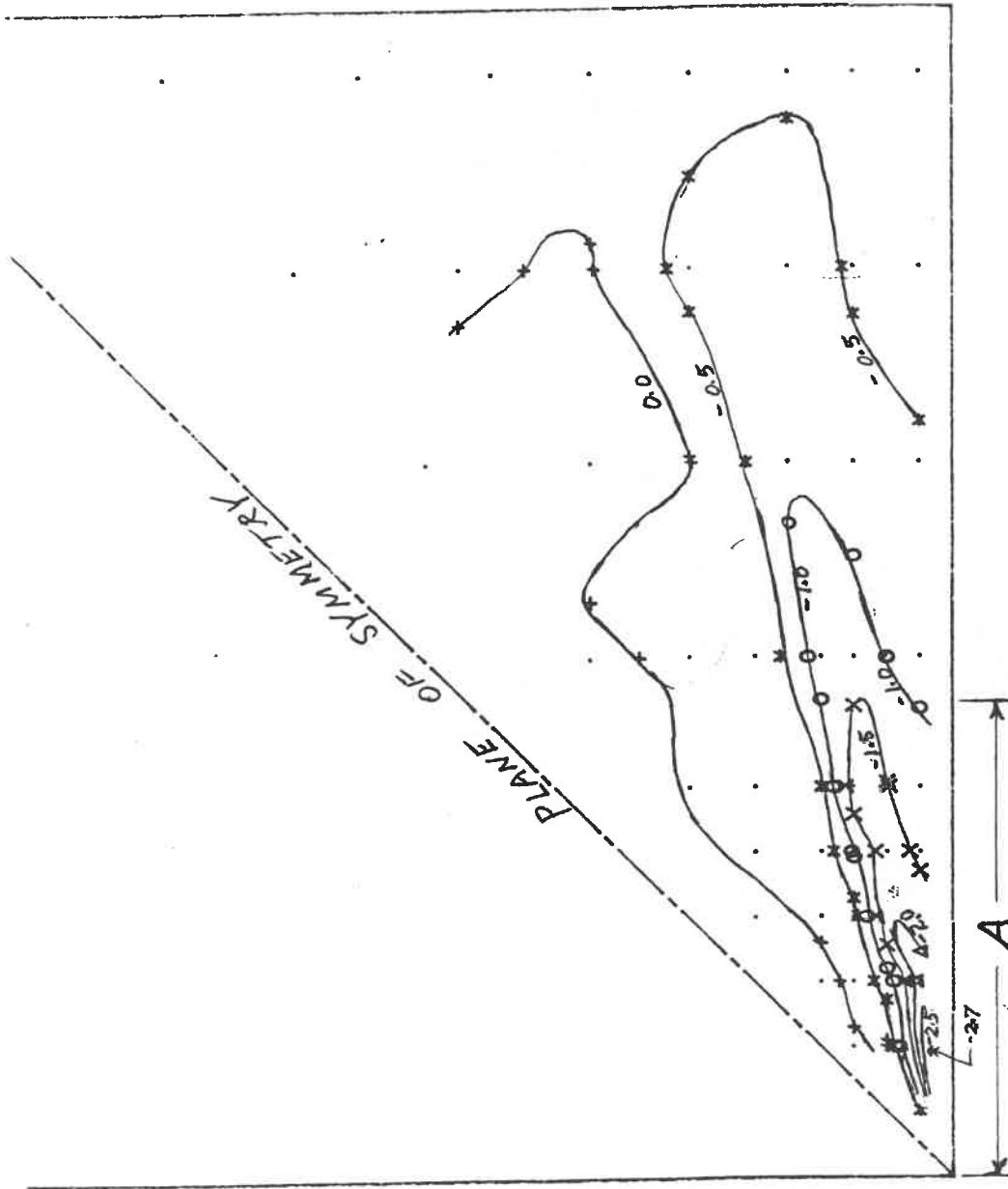


Figure 14 Pressure-Coefficient Contours for Configuration (viib) with  
9 1/2 in. wide by 6 3/8 in. high (2.65A x 1.8A) Open Jet  
(Optimum Jet Size)



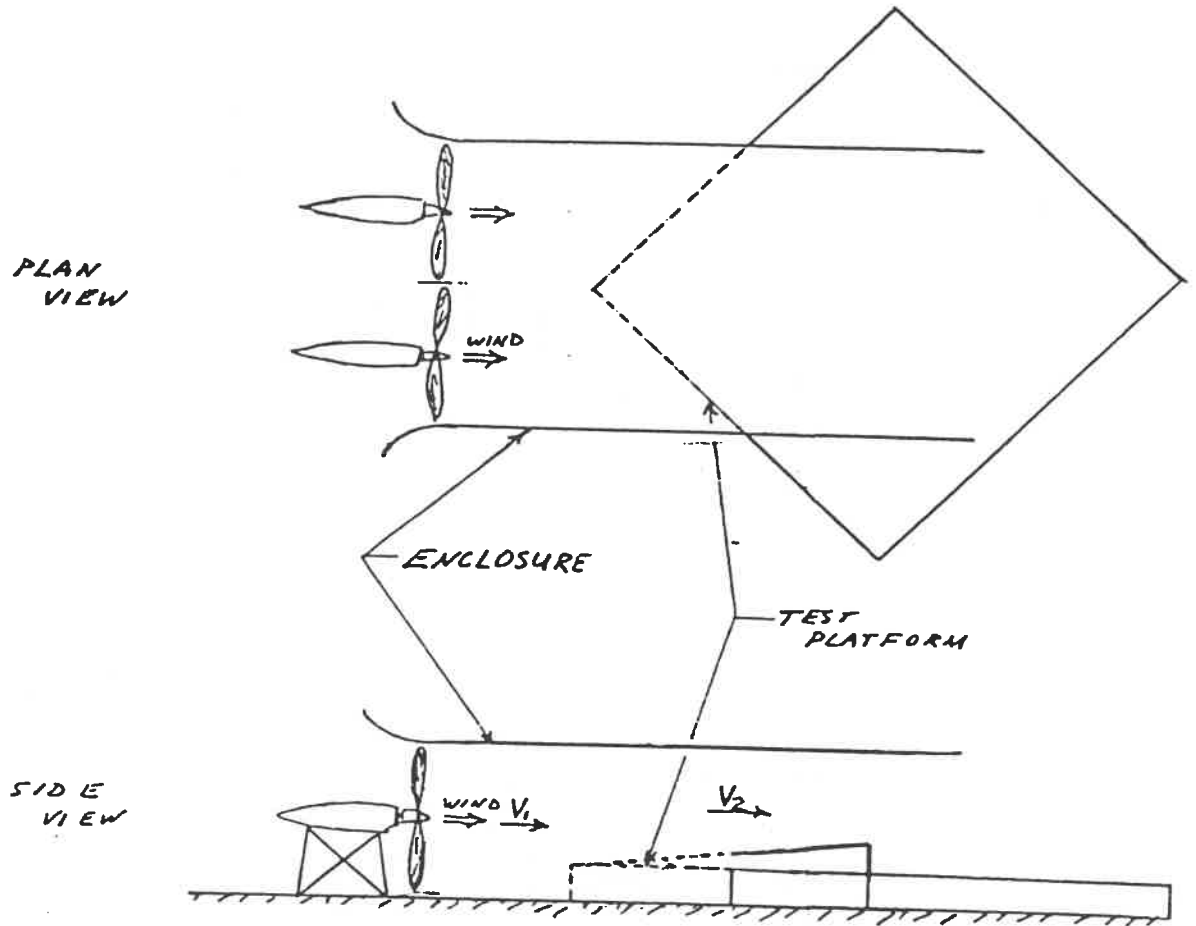


Figure 15 Schematic Sketch of Test Rig with Enclosure  
(Configuration (viii) of Table 1)

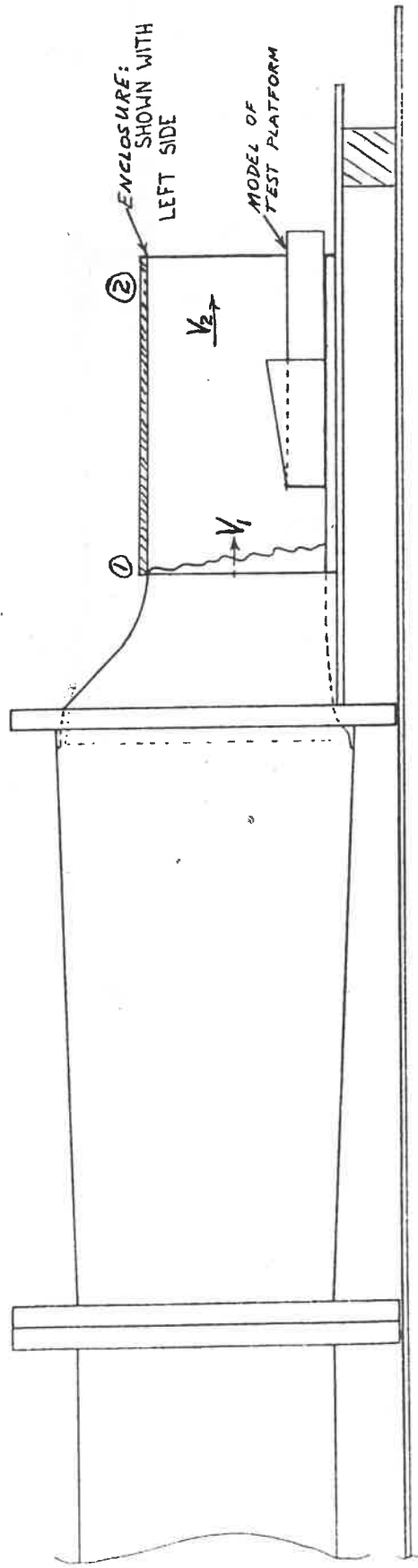


Figure 16 Set Up of Apparatus for Studies of Enclosed Jet Configurations

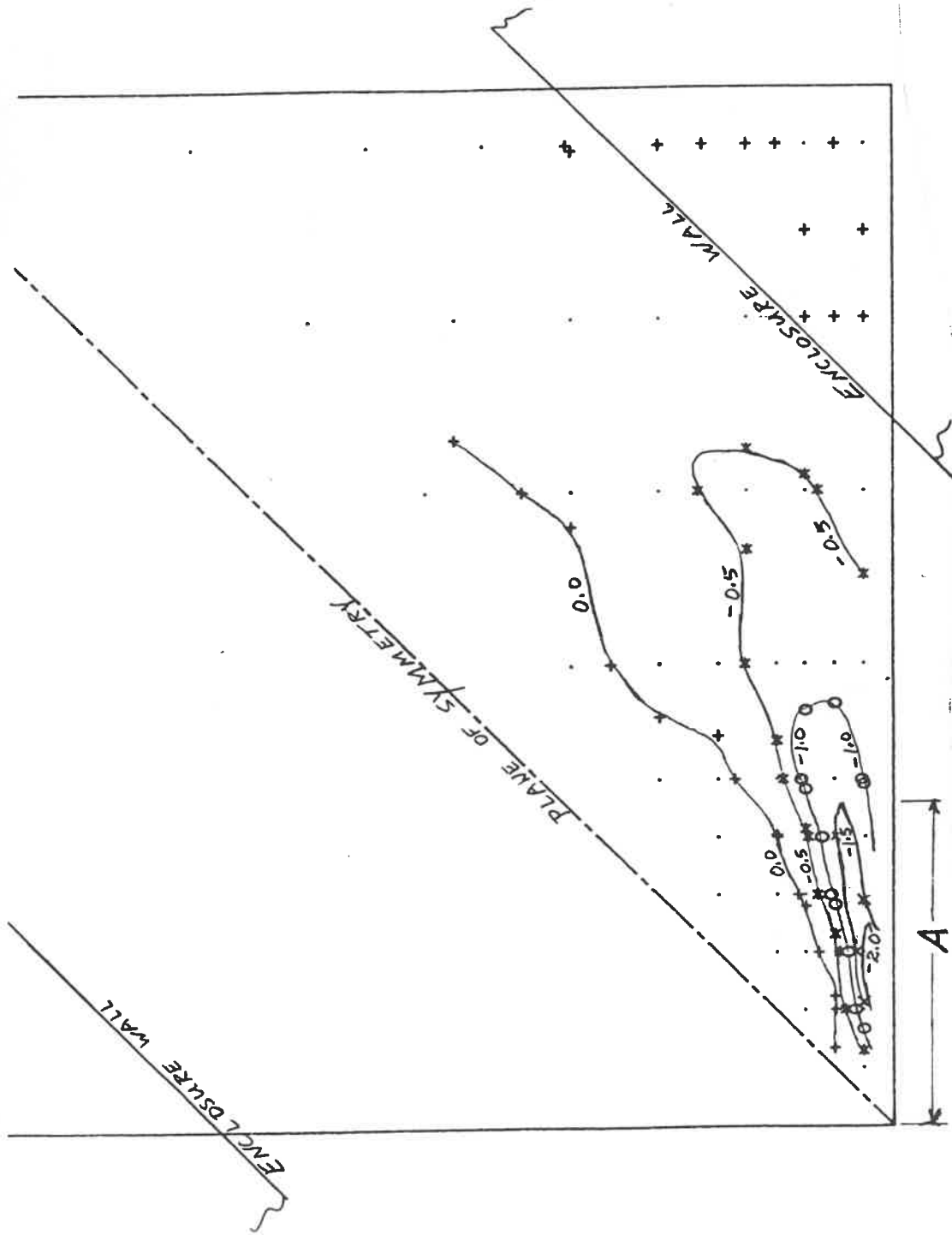


Figure 17 Pressure Coefficient Contours for Configuration (vilia) with 8 3/4 in. wide by 5 1/4 in. high (3.1A x 1.9A) Enclosed Jet (Optimum Jet Size)

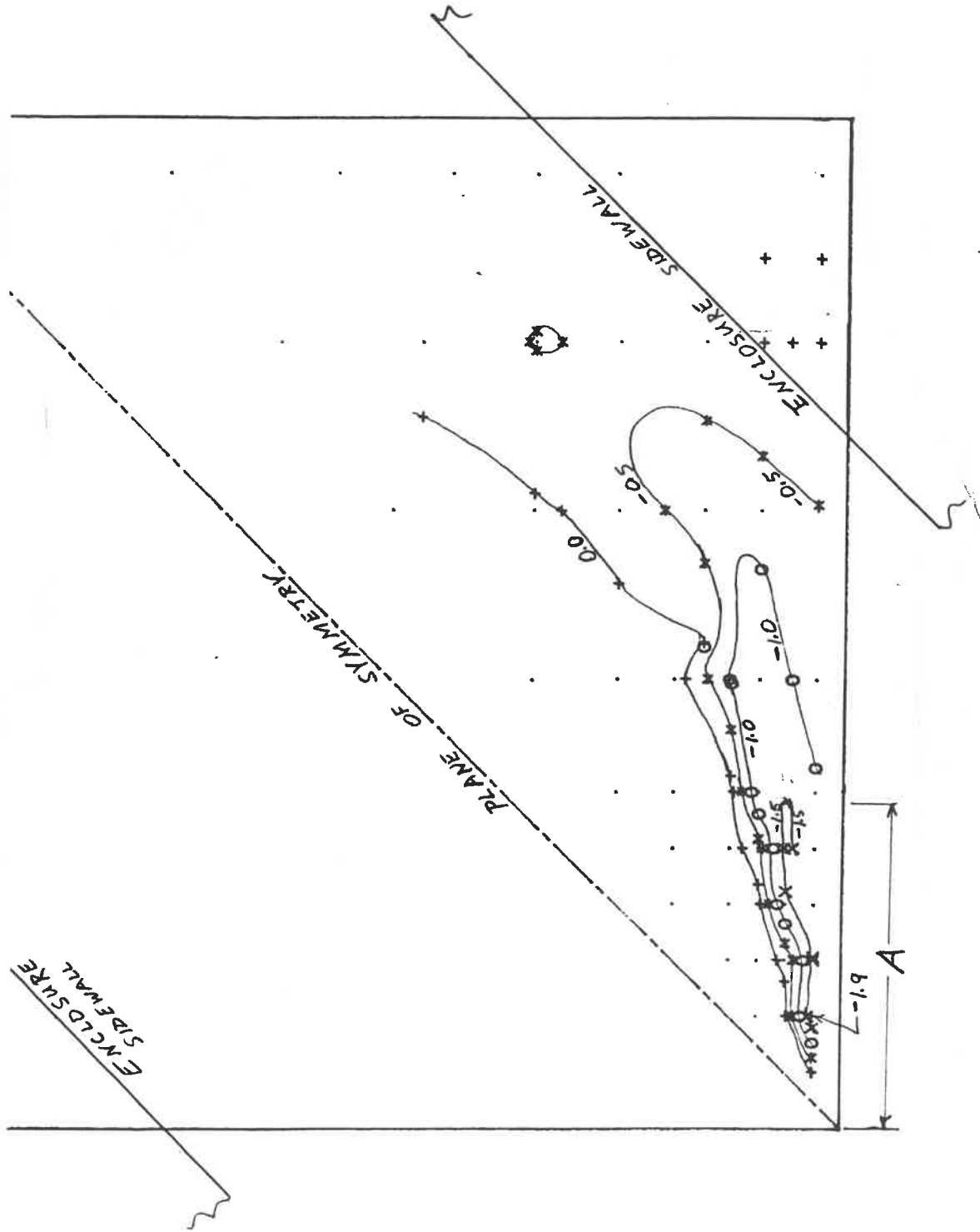


Figure 18 Pressure Coefficient Contours for Configuration (viiib) with 8 3/4 in. wide by 5 1/4 in. high (3.0A x 1.8A) Enclosed Jet (Optimum Jet Size)

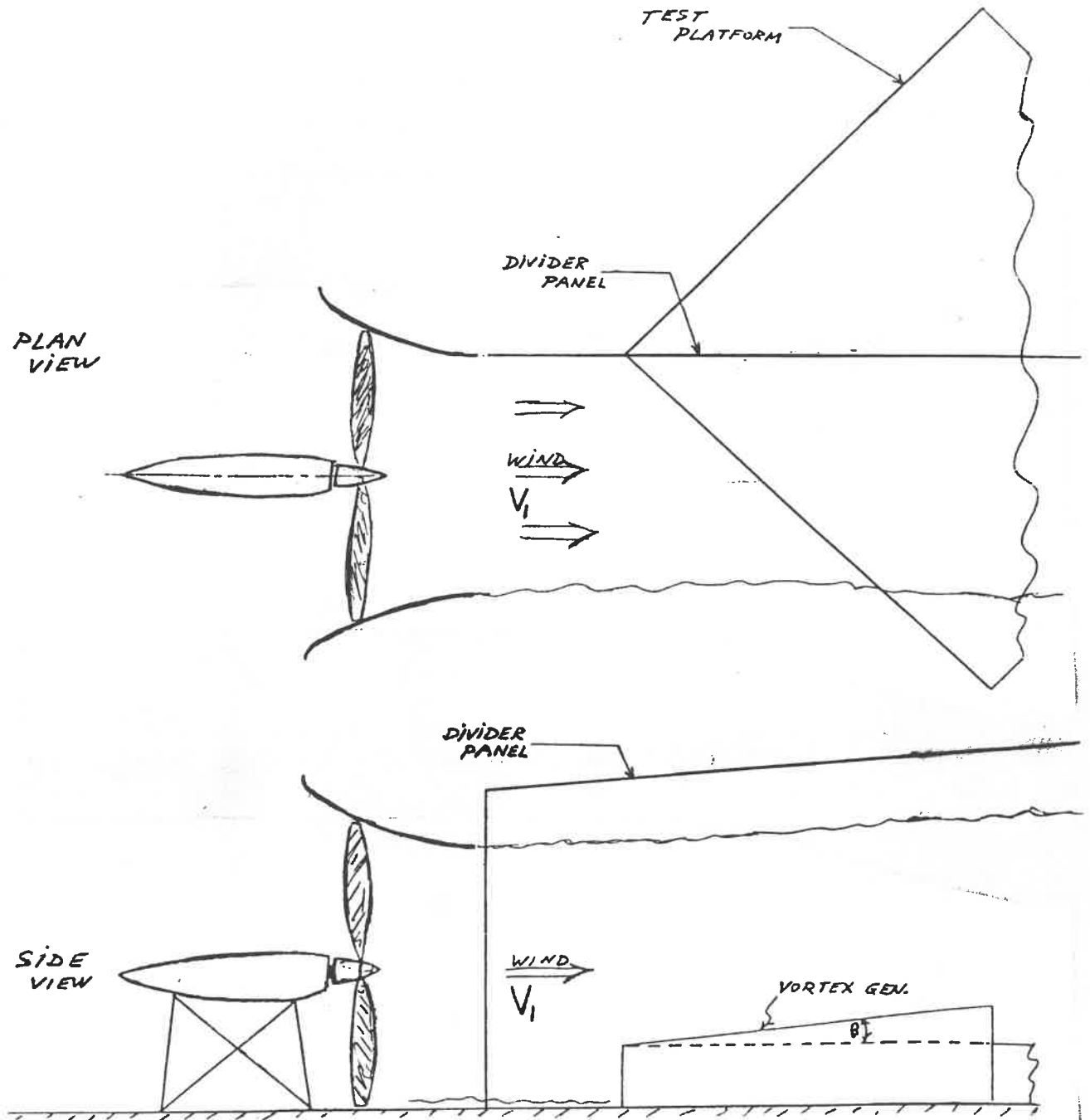


Figure 19 Arrangement of Divider Panel  
(Open Jet Configuration Shown)

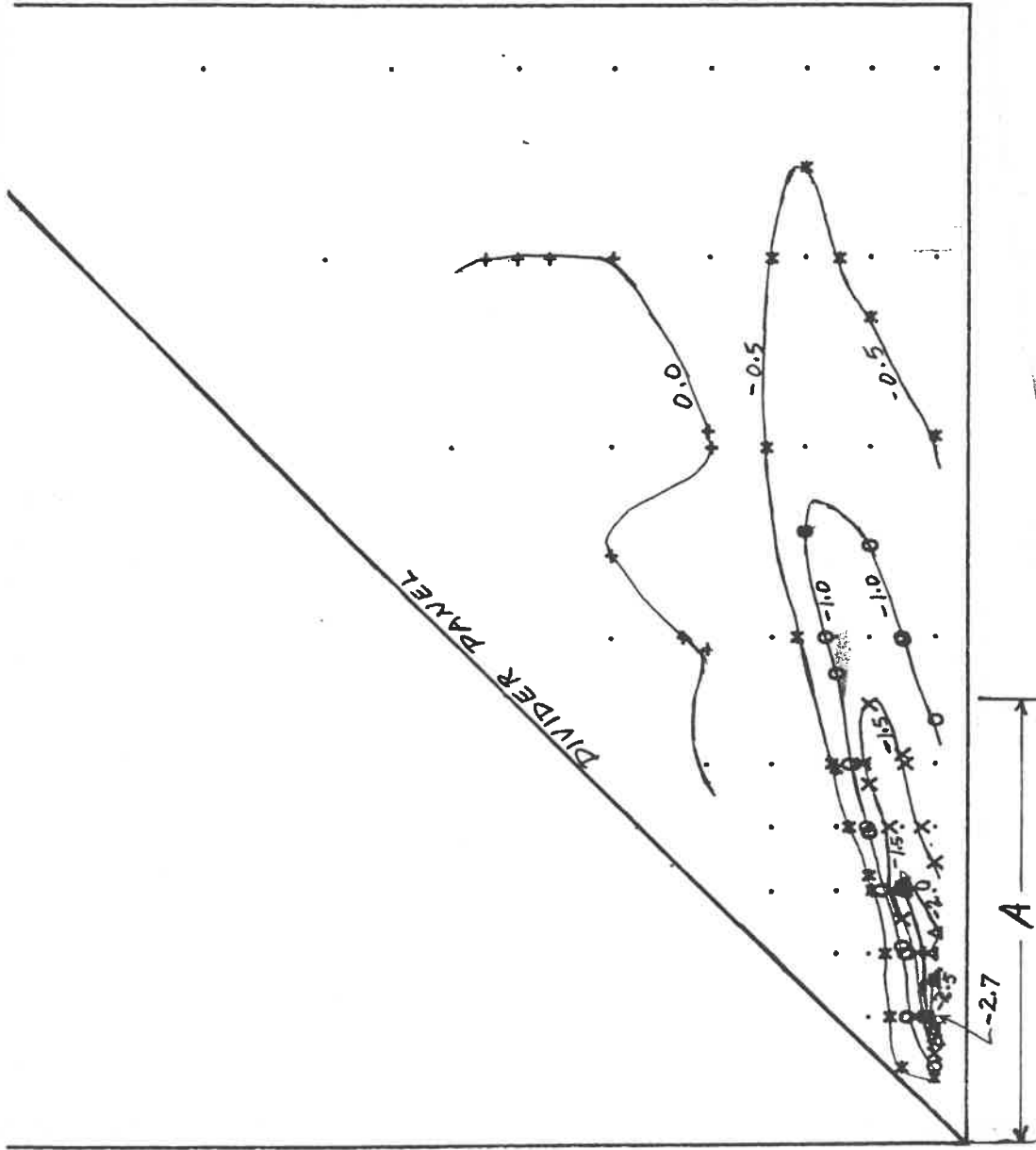


Figure 20 Pressure Contour Patterns for Configuration (ix) with  
4 3/4 in. wide by 6 3/8 in. high (1.35A x 1.8A) Open Jet  
(Optimum Jet Size)

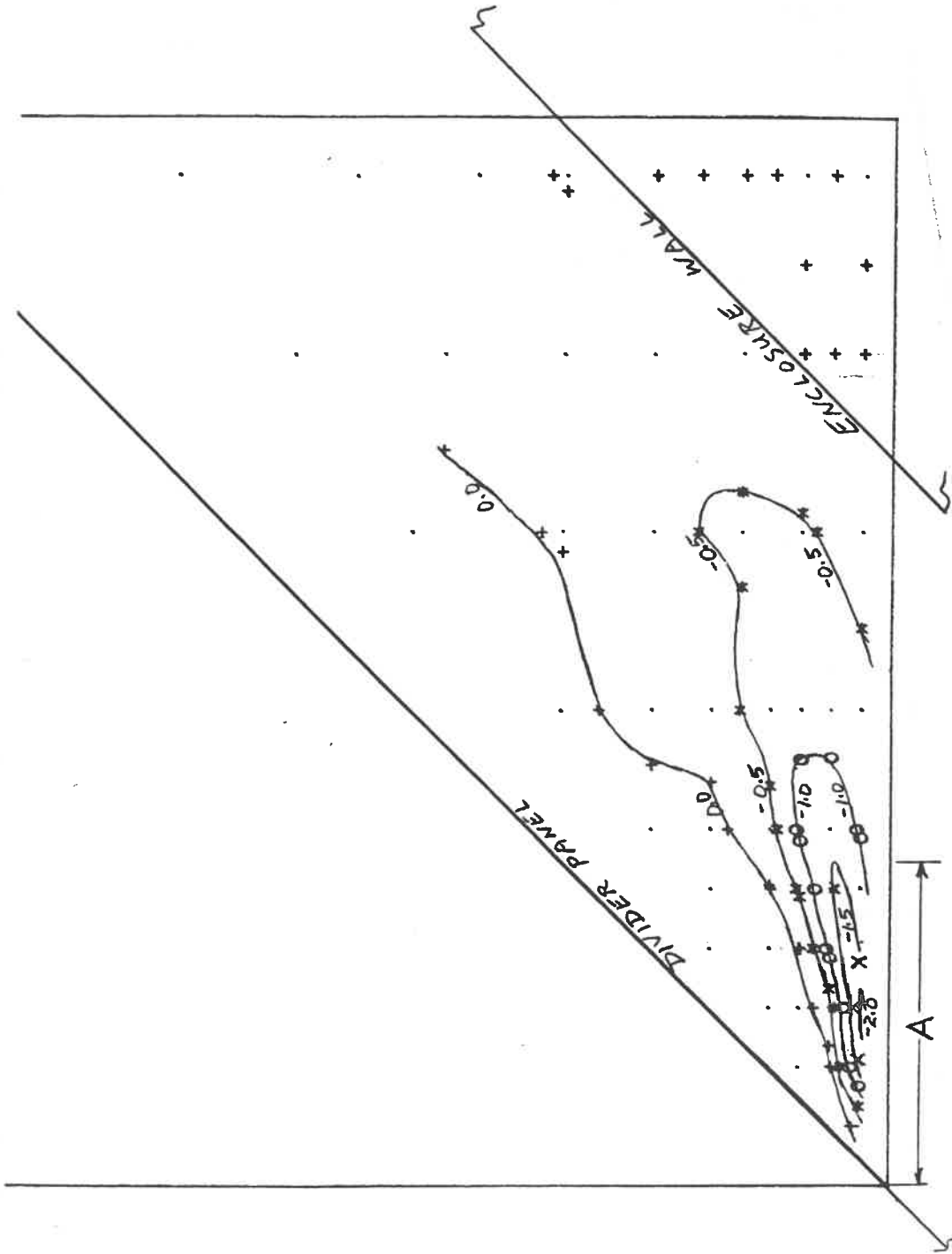


Figure 21 Pressure Coefficient Contours for Configuration (x) with  
4 3/8 in. wide by 5 1/4 in. high (1.6A x 1.9A) Enclosed Jet  
(Optimum Jet Dimensions)

APPENDIX

Breakdown of Cost Estimates of Table 2 (\$ US)



Appendix

Breakdown of Cost Estimates of Table 2 (\$U.S.)

Cost Item	Case A	Case B	Case C
Engine/propeller units air-starter system for engines, and piping, etc.	100,000 20,000	200,000 25,000	400,000 33,000
fuel supply system (pumps, pressure regulators, valves, piping)	25,000	35,000	55,000
fuel tank (5000 gal. per engine)(a)	10,000	20,000	40,000
concrete foundation slab (b)	30,000	35,000	85,000
engine mounting system	100,000	150,000	300,000
control and monitoring console	100,000	110,000	130,000
transition duct	250,000	350,000	1,300,000
test platform (c)	37,000	37,000	91,000
<b>TOTAL</b>	<b>\$672,000</b>	<b>\$962,000</b>	<b>\$2,434,000</b>

- (a) Each engine will consume about 380 U.S. gallons of fuel per hour when running at 4000 HP.
- (b) The test platform would be about 10 ft. high x 35 ft. x 35 ft. for Cases A, B and C, about 18 ft. x 55 ft. x 55 ft. for Cases D, E and F. The test platform would be on a concrete slab and would be similar in construction to a warehouse building. It would house the Control and Monitoring Console and provide storage facilities.
- (c) About 50 ft. x 100 ft. for Cases A and B; about 75 ft. x 150 ft. for Case E.